https://doi.org/10.1016/j.scitotenv.2016.06.214

Spatiotemporal variation of ozone precursors and ozone formation in Hong Kong: Grid field measurement and modelling study

X.P. Lyu[1], M. Liu[1], H. Guo*[1], Z.H. Ling[1], Y. Wang[1], P.K.K. Louie[2], C.W.Y. Luk[2]

1. *Air Quality Studies, Department of Civil and Environmental Engineering, The Hong Kong Polytechnic University, Hong Kong*
2. *Air Group, Hong Kong Environmental Protection Department, Hong Kong*

*Corresponding author. ceguohai@polyu.edu.hk

Abstract

Grid field measurements of volatile organic compounds (VOCs) covering the entire territory of Hong Kong were simultaneously carried out twice daily on 27 September 2013 and 24 September 2014, respectively, to advance our understanding on the spatiotemporal variations of VOCs and ozone (O_3) formation, the factors controlling O_3 formation and the efficacy of a control measure in Hong Kong. From before to after the control measure on liquefied petroleum gas (LPG) fueled vehicles, the VOCs originated from LPG vehicle exhaust deceased from 41.3 ± 1.2 μg/m^3 (49.7±1.5%) to 32.8±1.4 μg/m^3 (38.8±1.7%) (p<0.05). In contrast, the contribution to VOCs made by gasoline and diesel vehicle exhaust and solvent usage increased (p<0.05). VOCs and nitric oxide (NO) in LPG source experienced the highest reductions at the roadside sites, while the variations were not significant at the urban and new town sites (p>0.05). For O_3 production, LPG vehicle exhaust generally made a negative contribution (-0.17±0.06 ppbv) at the roadside sites, however it turned to a slightly positive contribution (0.004 ± 0.038 ppbv) after the control measure. At the urban sites, although the reduction of VOCs and NO was minor (p>0.05), O_3 produced by LPG vehicle significantly reduced from 4.19±1.92 ppbv to 0.95±0.38 ppbv (p<0.05). Meanwhile, O_3 produced by LPG at the new town sites remained stable. The analysis of O_3-precursor relationships revealed that alkenes and aromatics were the main species limiting roadside O_3 formation, while aromatics were the most predominant controlling factor at urban and new town sites. In contrast, isoprene and sometimes NO_x limited the O_3 formation in rural environment.

Keywords: VOCs; source apportionment; photochemical O_3; Eulerian box model; MCM

1 Introduction

Well known as a major air pollutant in the atmosphere, ozone (O_3) has attracted increasing concerns in recent years due to its adverse effects on human health, visibility and ecosystem (Louie et al., 2013; Wang et al., 2008). O_3 is formed by a series of complex photochemical reactions involving volatile organic compounds (VOCs) and nitrogen oxides (NO_x) in the presence of sunlight (Seinfeld and Pandis, 1997). Since photochemical O_3 formation has a nonlinear relationship with its precursors, *i.e.*, VOCs and NO_x, it is difficult to remediate the photochemical pollution, especially in the regions with frequently high O_3 events, such as the Pearl River Delta (PRD).

Continuously rapid urbanization and population growth in Hong Kong coupled with high surface VOCs and NO_x emission, high solar radiation and hot weather make this region a photochemically polluted area. Previous studies have reported that the photochemical O_3 formation in Hong Kong is generally VOC-limited (Cheng et al., 2010a, b; Zhang et al., 2007). Furthermore, a number of studies were carried out on the contributions to O_3 in Hong Kong of regional transport from PRD and superregional transport from eastern China (Xue et al., 2014; Li et al., 2012, 2013; Ling et al., 2013; Wang et al., 2009), and several efforts have been made to study formation mechanism of O_3 pollution in Hong Kong (Ling et al., 2014; Xue et al., 2014). Although Ling et al. (2014) revealed that photochemical reactivity and ozone production were absolutely different between a semirural site and an urban site in Hong Kong, there is little knowledge about the spatial patterns of the relationship between O_3 and its precursors.

In addition, a series of control measures have been implemented in Hong Kong to reduce VOCs emitted from different anthropogenic sources, including VOC-containing products, road transport and industry emissions to mitigate O_3 pollution (HKEPD, 2015a; Louie et al., 2013). Hence, grid field measurements pre- and post- a control measure would help assess the effectiveness of the measure. For example, promotion of LPG as a substitute fuel for taxi and public light buses in Hong Kong was the most striking measure to reduce VOC emissions in the

past decade. However, recently, LPG usage was found to become major contributor to ambient VOCs in Hong Kong due to poor maintenance (Lau et al., 2010; Ling et al., 2014). In general, the catalytic converters in the LPG-fueled vehicles should be replaced every 1-2 years, depending on maintenance and mileage. In Hong Kong, about 80% of taxis and 45% of public light buses using LPG as fuel have defective converters, resulting in excessive emissions of vehicle exhaust (HKEPD, 2013). As such, to reduce LPG-fueled vehicle emissions, the Hong Kong government set aside $150 million to replace the catalytic converters and associated components on LPG-fueled taxis and public light buses, which commenced in October 2013 and completed in April 2014. It is well known that properly functioning catalytic converters in the LPG-fueled vehicles could reduce emissions up to 90%.

Therefore, the objectives of this study were to evaluate the benefit of replacing catalytic converters and oxygen sensors on LPG-fueled vehicles, to examine the spatiotemporal variations of O_3 production by LPG, and to study the spatial characteristics of O_3-precursor relationships in Hong Kong.

2 Methodology

2.1 Grid sampling campaigns

Totally 30 sampling sites were selected in different districts covering the entire territory of Hong Kong. The grid measurement campaigns were conducted on 27 September 2013 and 24 September 2014, respectively. At each of the 30 sites, 3-minute VOC canister samples were collected once in the morning between 9:00 and 11:00 and another in the afternoon between 2:00 and 4:00. Two of the 30 sites had duplicate samples. In total, 64 samples were collected for each campaign. The 30 sites included 24 roadside sites and 6 general sites (Figure 1 and Table S1).

Thirteen out of the 30 sites were the Hong Kong Air Quality Monitoring Stations (AQMS) (http://epic.epd.gov.hk/EPICDI/air/station/) (Table 1), where trace gas data were available. These sites covered the entire territory of Hong Kong and could provide a full picture of photochemical O_3 formation. The 13 AQMSs were categorized into four types according to the land usage and

the distance from urban center, *i.e.*, 3 urban roadside sites, 5 urban sites, 4 new town sites and 1 rural site (Figure 1 and Table 1).

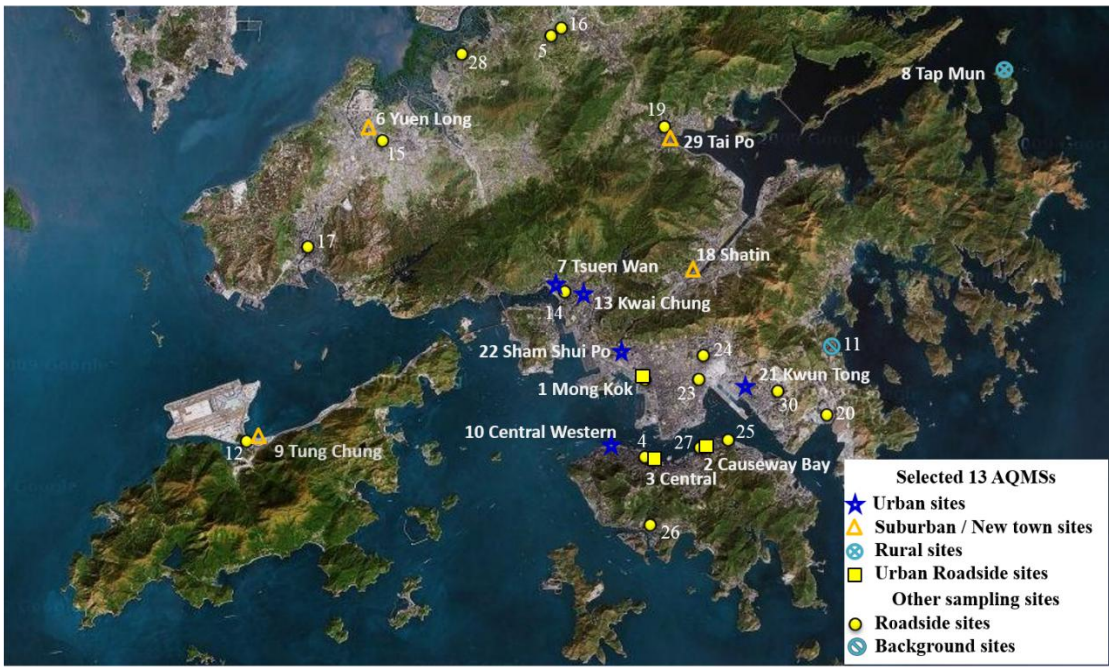

Figure 1 Geographic location of the sampling sites and surrounding environments.

Table 1 Description of the 13 AQMS sites

Type	Site	No.*	Description
Urban	Central Western (CW)	10	General urban air quality monitoring stations in residential areas and some mixed with commercial and/or industrial areas.
	Kwun Tong (KT)	21	
	Sham Shui Po (SSP)	22	
	Kwai Chung (KC)	13	
	Tsuen Wan (TW)	7	
Suburban/ New Town	Yuen Long (YL)	6	Mainly residential areas in new territories.
	Tung Chung (TC)	9	
	Tai Po (TP)	29	
	Sha Tin (ST)	18	
Rural	Tap Mun (TM)	8	Remote island off the northeast coast of Hong Kong
Roadside	Causeway Bay (CWB)	2	Commercial centers with high-rise buildings along the streets, high traffic and pedestrian flow, and frequent traffic jam in
	Central	3	

	Mong Kok (MK)	1	rush hours

* Sequence number in Figure 1.

2.2 Collection and analysis of VOC samples

Ambient VOC samples were collected using cleaned and evacuated 2 L electro-polished stainless steel canisters. The canisters were prepared and delivered to Hong Kong by the Rowland/Blake group at University of California, Irvine (UCI). A flow-controlling device was used to collect the samples for 3 minutes.

Before sampling, all canisters were cleaned at least five times by repeatedly filling and evacuating with humidified pure nitrogen gas (N_2). To test for any contamination in the canister, the evacuated canister was filled with pure N_2, stored for at least 24 h, then checked by the same VOC analytical methods to ensure that all the target compounds were not found or were under the method detection limit (MDL). In addition, duplicate samples were regularly collected to check the precision and reliability of the sampling and analytical methods. After sampling, the VOC samples were returned to the laboratory at UCI for chemical analysis. The analytical system, which was fully described in Simpson et al. (2010), used multicolumn gas chromatography (GC) with five column-detector combinations. The oven parameters employed for each GC can be found in Colman et al. (2001). In total, 39 non-methane hydrocarbons (NMHCs), methane (CH_4) and carbon monoxide (CO) were quantified from the canister samples. VOCs were identified via their retention time and mass spectra. The quantification of target VOCs was accomplished using multipoint external calibration curves, obtained from a combination of National Bureau of Standards, Scott Specialty Gases (absolute accuracy estimated to be within ±5 %) and UCI made standards. The detection limit, measurement precision and accuracy for each VOC varied and were listed in Simpson et al. (2010). Generally, alkanes, alkenes and aromatics had a detection limit of 3 pptv, a precision of 3%, and an accuracy of 5%.

For on-line measurements of VOCs, which were mainly used in section 2.5, a built-in computerized program, including auto-linearization, auto-calibration and calibration with span gas, was adopted to control the quality. The accuracy and precision of VOC measurements were 1.0-10.0% and 2.5-20.0 %, respectively.

2.3 PMF model

US EPA PMF model (version 5.0) was applied to the measurement data for receptor-based source appointment. The PMF model is a multivariate factor analysis tool that decomposes a matrix of speciated sample data into two matrices - factor contributions and factor profiles which can be interpreted by an analyst as to what sources are represented based on observations at the receptor site (Paatero, 1997; Paatero and Tapper, 1994).

The details of PMF applied to VOC data for source profiles and the contributions of individual VOC species have been introduced somewhere else (Guo et al., 2011a; Ling et al., 2011; Ou et al., 2015). Briefly, 18 NMHCs were input into the PMF model and the uncertainties for each sample/species were determined as the sum of 5-15% of VOC concentration and two times the method detection limit (MDL) of the species (USEPA, 2008). Values below the MDL were replaced by half of the MDL values and their overall uncertainties were set as 5/6 of the MDL values. Results were constrained so that no samples had negative source contributions. Different number of factors and uncertainties were tested, and an optimum solution was determined based on a good fit to the observed data and the most meaningful results by comparing with previous studies (Guo et al., 2011a, b; Lau et al., 2010).

2.4 Calculation of VOCs diurnal profiles

Since VOCs canister samples at the 30 sites were only collected at ~10:00 and 15:00, respectively, it was impossible to use them for a photochemical box modeling as the model required hourly data input for consecutive hours. Hence, it is necessary to derive time-dependent concentrations from the two canister samples for the use in the photochemical box model incorporating master chemical mechanism (PBM-MCM). The procedures to obtain hourly VOC

profiles from two samples were similar to the method described in Zhang et al. (2007). Briefly, the method was based on the mass conservation of a species inside a fixed Eulerian box, namely, the Eulerian box model (Seinfeld and Pandis, 1997). The entraining equations are:

$$\frac{dC_i}{dt} = \frac{q_i}{H(t)} + R_i - \frac{v_{d,i}}{H(t)} C_i + \frac{C_i^0 - C_i}{\tau_\gamma} \quad \text{for} \quad \frac{dH}{dt} \le 0 \qquad (1)$$

$$\frac{dC_i}{dt} = \frac{q_i}{H(t)} + R_i - \frac{v_{d,i}}{H(t)} C_i + \frac{C_i^0 - C_i}{\tau_\gamma} + \frac{C_i^a - C_i}{H(t)} \frac{dH}{dt} \quad \text{for} \quad \frac{dH}{dt} > 0 \qquad (2)$$

where, C_i: Concentration of species i (μg m^{-3}),

q_i : Emission rate of species i (μg m^{-2} s^{-1}),

$H(t)$: Mixing height as a function of time t (m),

R_i: Chemical destruction rate of species i (μg m^{-3} s^{-1}),

$\upsilon_{d,i}$: Dry/wet deposition rate of species i (m s^{-1}),

C_i^0: Background concentration of species i (μg m^{-3}),

τ_γ: Residence time of air over the area (s),

C_i^a: Concentration of species i above the boundary layer (μg m^{-3}).

Equations (1) and (2) mathematically describe the concentration of species above a given area, assuming that the corresponding airshed is well mixed, accounting for emissions, chemical reactions, removal, advection of material in and out of the airshed, and entrainment of material during growth of the mixing layer. Before the numerical solutions of equations (1) and (2) are solved with Gear's backward differentiation formula (Jacobson, 2005), the parameters in equations (1) and (2) need to be determined.

Emission Rates: the Hong Kong emission inventory of total anthropogenic VOCs from different sources in 2013 was used to estimate the annual emission amount (HKEPD, 2015b). This annual emission amount was then equally allocated to 52 weeks and the area of 1104 square kilometers covering Hong Kong territory. The area of Hong Kong was obtained from Censtatd (2016), while the days were classified as weekdays and weekends, and the emission factors of each day of a

week were determined by Cardelino (1998). Hence, the daily initial emission amount of total VOCs per unit area was calculated. This value was multiplied by the typical profile of ambient VOCs, which was obtained by averaging all canister data at different sites, to derive the daily initial emission rates of speciated VOCs at different sites. The diurnal variations of the anthropogenic VOC emissions were estimated according to source types. Industry and power generation were assumed to have no diurnal variations, while mobile emission had the same pattern as traffic flow in Hong Kong (Lam et al., 2006; Xia and Shao, 2005). The diurnal variation of biogenic VOCs (*i.e.*, isoprene) was estimated by considering the temperature variations and the best fit value coefficient T_M, which affected the predicted emission behavior at high temperatures (Guenther, 1993, 1999). In this way, the speciated VOCs emission rates from different sources were determined.

Mixing Height Profile: The mixing height was estimated using the Holzworth method (Holzworth, 1967). The Holzworth method provides twice-per-day (morning and afternoon) mixing heights based on calculations using routine upper-air data and minimum and maximum temperature of the day. The upper air sounding data were obtained from the University of Wyoming (http://weather.uwyo.edu/upperair/sounding.html). The minimum temperature was determined from the data of King's Park station operated by Hong Kong Observatory (HKO) (http://www.hko.gov.hk/) for the time period of 0200-0600 local standard time (LST). Here, we followed the method of Zhang et al. (2007), which also calculated the mixing height in Hong Kong by using "plus 2 °C" to the morning minimum surface temperature to calculate the morning mixing height. The afternoon mixing height was calculated using the maximum surface temperature observed at 1200-1600. The hourly mixing heights, often used in regulatory dispersion modeling, were interpolated from these twice-per-day estimates. The recommended interpolation procedure is provided in the user's guide for the Industrial Source Complex (ISC) dispersion model (USEPA, 1985).

The dry/wet deposition rate and the concentration above the boundary layer were assumed to be

zero for all VOCs. Background concentrations of VOCs were expressed as geometric mean concentrations at general sites. Residence time of air over the area was the ratio of length of the box to wind speed, and the time-dependent wind speed was determined by curve fitting using the in-situ hourly wind speed obtained from the HKO. Since length of the box and emission rates of VOCs at different sites were different and the VOC chemical destruction rates were unknown, we adopted an iterative approach to determine these parameters based on canister data at 10:00 and 15:00. We first used a typical OH profile in clean marine atmosphere (Creasey et al., 2003) and the initial emission rate of propane to calculate the temporal variations of propane from 10:00 to 15:00 with the box length ranging from 0 to 60 km (*i.e.*, beyond the longest range of Hong Kong territory). Propane was selected due to its high concentration and lower reactivity with OH compared to alkenes. The optimal emission rate and the length of box were adjusted by matching the calculated propane level at 15:00 with the observed value, using a 5% agreement for consistency. The ratio of optimal emission rate to initial emission rate of propane was defined as emission rate factor. The temporal variation of more reactive propene from 10:00 to 15:00 was calculated in the same way, but the length of box was fixed and the emission rate of propene was modified by multiplying the initial emission rate of propene by the emission rate factor determined by propane above. As such, the original OH profile used above was refined to fit the real situation in Hong Kong. The refined OH profile was then used to recalculate the temporal variation of propane. The entire procedure was called iteration. Iterations were repeated until convergence was obtained. Thus the length of box, emission rates of VOCs and OH profiles at different sites were obtained via this iterative approach.

2.5 PBM-MCM model

The photochemical box model (PBM) incorporating Master Chemical Mechanism (MCM) is a near-explicit chemical mechanism which describes the detailed gas-phase chemical processes involving the tropospheric degradation of a series of primary VOCs. The chemical mechanistic information was extracted from the Master Chemical Mechanism, MCM v3.2 (Jenkin et al., 1997;

Saunders et al., 2003), via website http://mcm.leeds.ac.uk/MCM.

The model was constructed with measured CO, NO, NO_2, SO_2, C_2-C_9 NMHCs, temperature and relative humidity. Data were read every hour to calculate the in-situ rates of O_3 production and destruction. The model has been widely used in Hong Kong (Ling et al., 2014; Lyu et al., 2015b, 2016).

3 Results and discussion

3.1 Meteorological conditions

Figure 2 shows the average geopotential height (HGT) and wind field on 1000 hPa for East Asia during the two sampling campaigns. The pressure (represented with HGT) over Hong Kong was comparable between the two campaigns. The wind was northeasterly on 27 September 2013, while it was calm on 24 September 2014 in Hong Kong. The lower wind speed in the latter campaign was expected to elevate the VOC concentrations. However, the levels of most VOCs remained similar, whereas those emitted from LPG source decreased between the two campaigns (see sections 3.2 and 3.3), indicating that meteorological parameters did not have substantial influence on the VOC levels of the two campaigns.

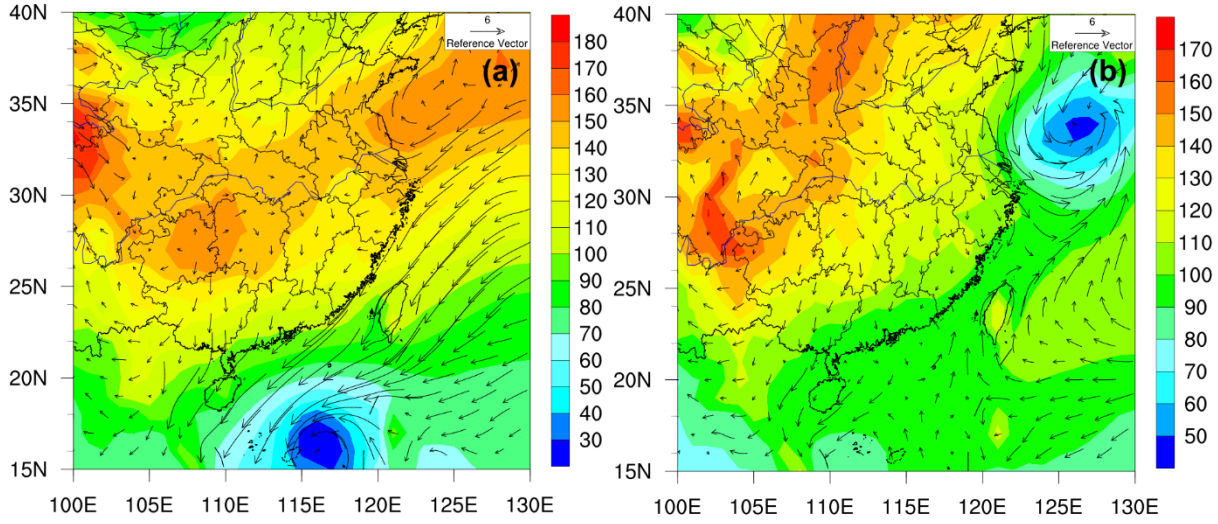

Figure 2 Average geopotential height and wind field on (a) 27 September 2013 and (b) 24 September 2014. The figures are made using NCEP FNL (final) data with a horizontal resolution of 1°×1°.

3.2 Comparison of VOCs between the two campaigns

Table 2 presents the average mixing ratios of VOCs at the 24 roadside sites and 6 general sites during the two campaigns. It is noteworthy that the average VOC values for the sites should reflect the real situation though uncertainties could exist for the samples at individual sites. It was found that the alkanes dominated the total VOC composition, followed by aromatics and alkenes, and the mixing ratios at roadside sites were much higher than those at general sites due to their proximity to the emission sources (p<0.05). From September 2013 to September 2014, values of most species remained unchanged except for *n*/*i*-pentanes, which increased at the general sites (p<0.05), indicating possibly increased emission of gasoline-fueled vehicles. Furthermore, aromatics such as xylenes and propylbenzenes increased significantly (p<0.05), perhaps due to the increase of solvent usage and/or vehicular emissions. In contrast, LPG related VOCs (propane and *n*/*i*-butanes) remained unchanged, while propene, the tracer of LPG combustion, even decreased at the roadside sites (p<0.05). In view of the above fact, to examine whether the replacement program was actually effective, it is necessary to conduct source apportionments to obtain the emission variations of LPG-fueled vehicles before and during the replacement program.

Table 2 Mixing ratio of VOCs collected at the 30 sampling sites during the 2 sampling campaigns (average±95% confidence interval, pptv)

	Species	Roadside sites (n=24) [a]		General sites (n=6) [a]	
		Sept. 2013	Sept. 2014	Sept. 2013	Sept. 2014
Alkanes	Ethane	2518±209	2704±206	1833±179	1884±280
	Propane	7723±1872	6996±1039	3631±2478	2849±1076
	n-Butane	11166±3104	9003±1645	2828±1876	2694±1247
	i-Butane	6413±1726	5455±931	1866±1227	1762±799
	n-Pentane	773±197	1209±457	331±74	866±321 *
	i-Pentane	1331±324	2097±1127	608±112	1372±499 *
	n-Hexane	323±92	529±86 *	148±42	415±177 *
	2,3-Dimethylbutane	118±46	186±51	48±22	137±58 *
	2-Methylpentane	593±193	847±223	301±137	754±408
	3-Methylpentane	315±95	588±153 *	174±85	552±285 *
	n-Heptane	437±242	480±122	122±35	226±93 *
	2-Methylhexane	444±235	416±82	151±51	255±123

	3-Methylhexane	449±243	510±90	145±51	353±156 *
	n-Octane	106±37	137±46	47±10	74±24
	2,2,4-Trimethylpentane	255±132	316±81	37±8	109±66 *
Alkenes	Ethene	4631±917	3748±669	1097±327	1082±398
	Propene	1798±417 *	1084±230	233±70	201±93
	1-Butene	197±40	161±32	53±21	48±25
	i-Butene	566±145 *	371±87	150±58	94±33
	trans-2-Butene	132±36	99±26	20±8	21±8
	cis-2-Butene	82±25	56±15	14±4	13±5
	1-Pentene	55±11	93±49	19±6	28±11
	1,3-Butadiene	149±37	119±24	29±5	17±10
	Isoprene	531±90	627±115	500±230	777±285
Alkyne	Ethyne	3916±671	3375±391	1978±426	2037±404
Aromatics	Benzene	886±138 *	662±64	556±67	518±105
	Toluene	3270±1751	3371±527	1634±610	2745±1136
	Ethylbenzene	643±127	674±87	438±150	703±230
	p-Xylene	291±85	420±69 *	130±39	378±163 *
	m-Xylene	483±178	703±153	161±50	602±296 *
	o-Xylene	337±103	471±79	142±44	428±180 *
	i-Propylbenzene	39±13	42±6	17±4	34±10 *
	n-Propylbenzene	92±39	79±14	30±9	53±16 *
	3-Ethyltoluene	380±210	212±59	66±23	113±47
	4-Ethyltoluene	187±112	119±28	37±10	75±30 *
	2-Ethyltoluene	164±76	87±22	41±12	53±22
	1,3,5-TMB	234±127 *	78±24	40±14	37±15
	1,2,4-TMB	821±486 *	288±85	128±54	145±67
	1,2,3-TMB	228±102	84±22	56±24	45±19

[a] Number of sites; * higher mixing ratios as compared to those in another sampling campaign at the confidence level of 95% (p<0.05). TMB refers to the trimethylbenzene isomers hereafter.

3.3 Source apportionments of VOCs and trace gases

Twenty main anthropogenic VOC species quantified in the 64 samples were applied to PMF for source apportionment for the two campaigns, respectively. The source profiles before and after the intervention program are similar (Figure 3). Three factors were extracted from the PMF model simulation. Since most of the samples were collected at roadside sites, it is expected that vehicular emissions were the dominant sources of VOCs in this study. The first factor was distinguished by the dominance of propane, *n*/*i*-butanes, ethene and propene, representing LPG-fueled vehicle exhaust. Factor 2 had high percentages of all VOCs and trace gases except LPG related component and the trimethylbenzene isomers. It was assigned as gasoline and diesel vehicle exhaust. The third factor was closely associated with solvent usage because of high

loadings of xylenes and trimethylbenzenes. The profiles of factors identified were based on the results of previous source apportionment studies (Guo et al., 2007, 2011a; Lau et al., 2010; Ling et al., 2011) and VOCs source emission studies (Borbon et al., 2002; Guo et al., 2006, 2011b; Ho et al., 2009). Many different starting seeds were tested and no multiple solutions were found. In addition, good correlations were found between the observed and predicted VOC concentrations for the whole dataset (R^2 = 0.95 and 0.96, respectively) before and after the replacement program. Moreover, all of the selected species had scale residuals normally distributed between -3 and 3, confirming that the measured data were well reproduced (USEPA, 2008).

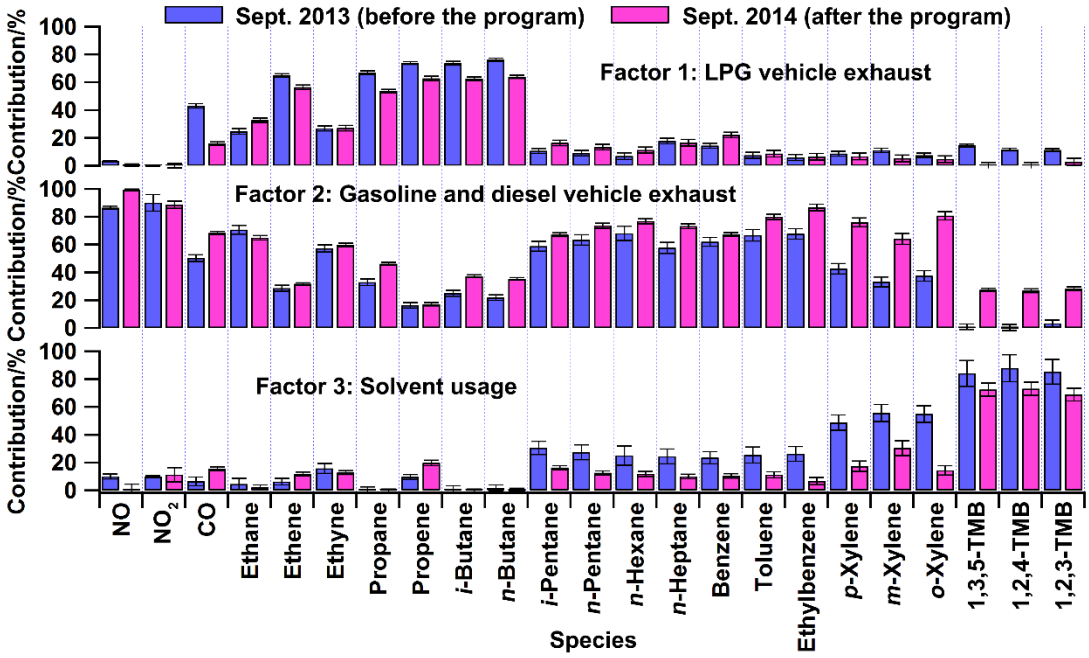

Figure 3 Source profiles of the three sources extracted from PMF in September 2013 (before the program) and September 2014 (after the program). The standard errors are estimated with the bootstrap in the PMF model.

To sum up the VOC concentrations in each source, the mass and percentage contributions of the sources to VOCs are summarized in Table S2. Noticeably, the vehicle emissions were the dominant source of VOCs, with the contribution of 71.1±1.8 μg/m^3 (85.5±2.1%) and 77.7±1.3 μg/m^3 (92.0±1.6%) before and after the program, respectively. From 2013 to 2014, the VOCs emitted from gasoline and diesel vehicles increased remarkably (p<0.05), whereas those

originated from LPG vehicle exhaust decreased significantly (p<0.05) from 41.3±1.2 μg/m^3 (49.7±1.5%) to 32.8±1.4 μg/m^3 (38.8±1.7%). Table 3 shows the average concentrations of VOCs and trace gases in LPG vehicle exhaust. Clearly, CO, ethene, propane, propene, *n*/*i*-butanes and trimethylbenzene isomers all reduced significantly from before to after the replacement program (p<0.05). The emissions of NO and NO_2 from LPG-fueled vehicles were minor, and the decrease of NO was insignificant (p>0.05). Table 4 presents the reductions of VOCs and NO at different sites. The mass and percentage contribution of LPG vehicle exhaust to VOCs experienced the greatest decrease at the roadside sites (p<0.05), with the contributions of 54.7±23.2 μg/m^3 (54.6±10.0%) before and 25.0±11.2 μg/m^3 (30.8±9.9%) after the program, respectively. The effects were much weaker at the urban and new town sites, where the mass and percentage contribution to VOCs decreased slightly or even increased (p>0.05). Similarly, NO decreased noticeably (p<0.05) (before: 0.66±0.28 μg/m^3; after: 0.04±0.02μg/m^3) at roadside sites, while the reductions were not significant at the urban and new town sites (p>0.05). This inter-site difference was possibly caused by higher traffic flow and more dense LPG-fueled vehicles (particularly taxis) in the vehicle fleet at roadside sites.

Table 3 Concentrations of VOCs and trace gases emitted from LPG-fueled vehicles (μg/m^3)

Species	LPG vehicle exhaust	
	before	after
NO	0.49 ± 0.44	0.03 ± 0.44
NO_2	0.00 ± 0.94	0.00 ± 1.05
CO	**336.24 ± 12.71**	**149.5 ± 11.1**
Ethane	0.71 ± 0.06	1.03 ± 0.05
Ethene	**2.83 ± 0.05**	**2.00 ± 0.05**
Ethyne	0.89 ± 0.06	0.87 ± 0.07
Propane	**7.63 ± 0.16**	**6.07 ± 0.14**
Propene	**1.76 ± 0.02**	**0.91 ± 0.02**
***i*-Butane**	**8.93 ± 0.16**	**6.98 ± 0.13**
***n*-Butane**	**16.00 ± 0.26**	**11.52 ± 0.20**
i-Pentane	0.30 ± 0.05	0.75 ± 0.09
n-Pentane	0.14 ± 0.03	0.38 ± 0.06
n-Hexane	0.05 ± 0.02	0.17 ± 0.03
n-Heptane	0.14 ± 0.01	0.20 ± 0.03
Benzene	0.37 ± 0.05	0.44 ± 0.04
Toluene	0.56 ± 0.16	0.94 ± 0.25
Ethylbenzene	0.13 ± 0.05	0.17 ± 0.06

p-Xylene	0.08 ± 0.02	0.10 ± 0.04
m-Xylene	0.14 ± 0.02	0.11 ± 0.05
o-Xylene	0.08 ± 0.02	0.08 ± 0.04
1,3,5-TMB	**0.12 ± 0.01**	**0.00 ± 0.01**
1,2,4-TMB	**0.32 ± 0.03**	**0.00 ± 0.03**
1,2,3-TMB	**0.11 ± 0.01**	**0.01 ± 0.01**

Bolded are the species with significant reduction in LPG vehicle exhaust (p<0.05).

Table 4 Mass and percentage contribution of LPG vehicle exhaust to VOCs and NO at different sites before and after the program

Species	Site	Mass concentration (μg/m^3)		Percentage contribution (%)	
		before	after	before	after
VOCs	Urban roadside	54.7 ± 23.2	25.0 ± 11.2	54.6 ± 10.0	30.8 ± 9.9
	Urban	28.7 ± 35.8	23.7 ± 11.8	29.3 ± 30.3	31.1 ± 10.5
	New town	11.5 ± 9.8	16.5 ± 17.1	27.9 ± 23.6	20.8 ± 20.3
NO	Urban roadside	0.66 ± 0.28	0.02 ± 0.01	0.04 ± 0.02	0.005±0.002
	Urban	0.34 ± 0.42	0.02 ± 0.02	0.03 ± 0.03	0.005±0.004
	New town	0.14 ± 0.12	0.02 ± 0.02	0.01 ± 0.01	0.003±0.004

3.4 Impact of replacement program on O_3 formation

3.4.1 Model validation and O_3 simulation

Since the estimated diurnal profiles of VOCs were used to simulate O_3, it is necessary to validate the results with the online measured VOCs. Figure 4 shows the estimated and online measured diurnal patterns of total VOCs at MK, YL and TC, where the real-time VOCs data were available. 26 VOC species were included in the total VOCs for calculation. The diurnal patterns of total VOCs estimated from the two points of canister sample data agreed well with the real-time measurements. Table S3 lists the Index of Agreement (IOA) values between the calculated and measured data of the 26 VOC species. Within the range of 0~1, higher IOA value indicates better agreement (Wang et al., 2015; Jiang et al., 2010). Fair to good agreement between the calculated and measured profiles of individual VOCs at these three types of sites suggested that the proposed method provided a reasonable estimate of VOC profiles based on the two canister samples. It is noteworthy that the measured and estimated VOC profiles during 01:00-09:00 did not fit very well at MK, probably due to the fact that the concentrations of VOCs, on one hand, were significantly influenced by in-situ traffic emissions as MK was a roadside site. On the other

hand, the method for estimating VOC diurnal profiles in this study was based on emission inventory, which was an averaged profile. This discrepancy in early morning would not substantially influence the simulation of O_3 formation, because O_3 formation was mainly simulated at daytime hours (*i.e.*, 07:00~19:00), and the photochemical reactions of VOCs were weak between 01:00 and 09:00.

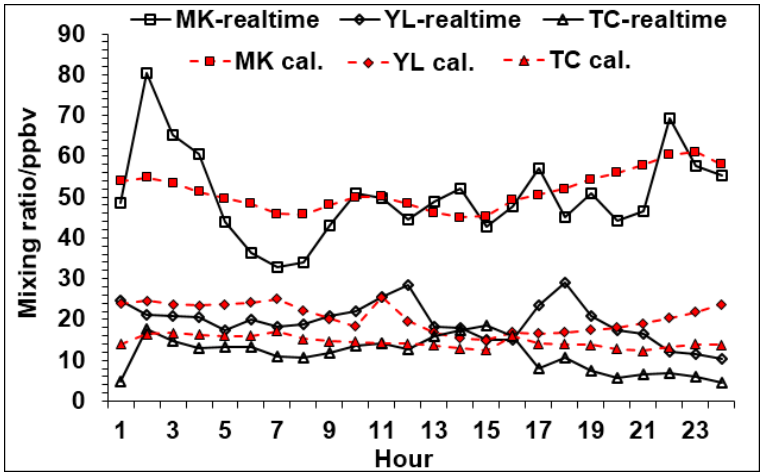

Figure 4 Estimated and real-time measured diurnal profiles of total VOCs at MK, YL and TC.

The calculated VOC diurnal profiles were then input into the PBM-MCM model for O_3 simulation. Figure 5 shows the daytime (07:00~19:00) simulated and observed O_3 in 2013 and 2014 at 13 sites where the online data of trace gases were available from the air quality monitoring network of HKEPD. In general, the simulated O_3 agreed well with the observations, with the consistence of the peaks and troughs. The IOA between the simulated and observed O_3 was 0.7, indicating fairly acceptable performance of the model. In other words, in-situ O_3 formation dominated its ambient level at most sites. The difference between model simulation and observation at some other sites was likely due to the fact that the PBM-MCM model only considers O_3 produced from photochemical reactions while the observed O_3 is also influenced by the downward transport of stratospheric O_3, dry deposition and horizontal transport from other regions/locations (Cheng et al., 2010a; Creilson et al., 2003; Lam et al., 2013; Xue et al., 2011).

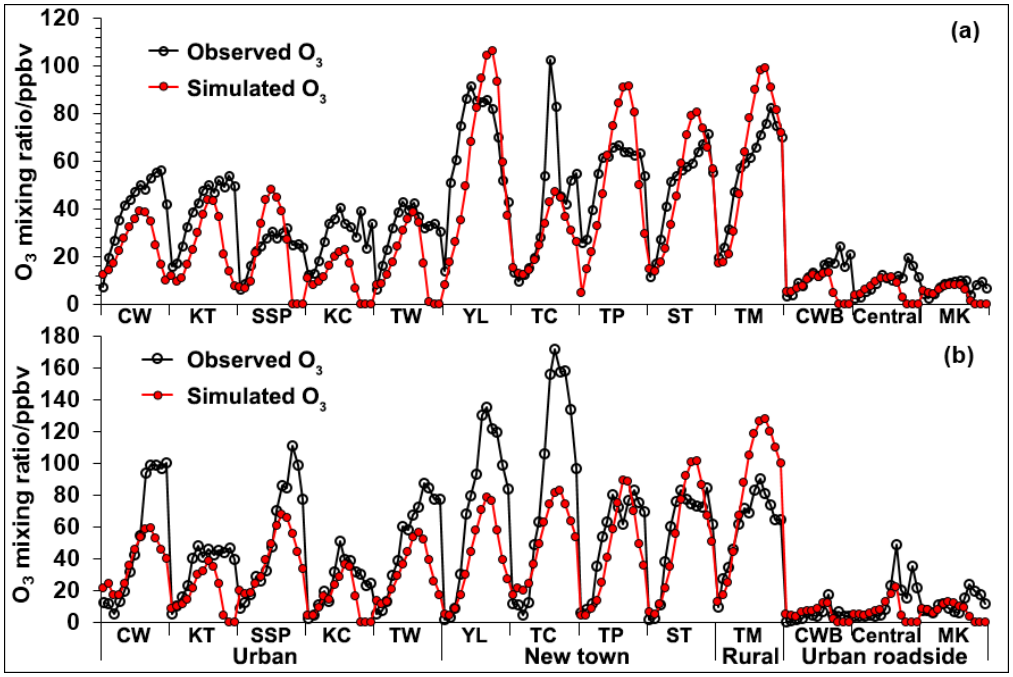

Figure 5 Comparison between simulated and observed O_3 in (a) September 2013 and (b) September 2014.

3.4.2 Impact of the program on O_3 formation

Given the reduction of VOCs and NO emitted from LPG-fueled vehicles, it is interesting to explore the impact of these changes on O_3 formation at different sites.

Sensitivity experiments give the differences in O_3 production between the scenarios with and without the LPG source as input. Through this approach, the O_3 produced by LPG source before and after the program were obtained (Figure 6). Since O_3 formation was usually limited by VOCs and suppressed by NO titration, the VOCs and NO in LPG made positive and negative contributions to O_3 production, respectively. Considering the combined effect of VOCs and NO on O_3 formation, LPG generally made a net positive contribution to O_3. However, the contribution of LPG vehicle to O_3 formation at roadside sites was negative before the program, mainly due to higher levels of NO emitted from LPG-fueled vehicles (0.66±0.28 μg/m^3) than those at urban (0.34±0.42 μg/m^3) and new town sites (0.14±0.12 μg/m^3), resulting in higher NO titration to O_3.

Table 5 lists the average contributions of LPG vehicle exhaust to O_3 at different types of sites

before and after the replacement program. At the roadside sites, the contribution of LPG vehicle turned from O_3 destruction (-0.17±0.06 ppbv) before to O_3 formation (0.004±0.038 ppbv) after the program. However, the resulting O_3 increase was minor (only 0.18 ppbv, 3.1% of the average roadside O_3 value). Although the decrease of VOCs and NO was not significant at the urban sites (p>0.05), O_3 produced by LPG source decreased significantly (p<0.05), reflecting nonlinear relationship between O_3 and its precursors, and also indicating the effectiveness of the program on O_3 production at urban sites. At the new town sites, no significant change in the contribution of LPG vehicle to O_3 production were observed (p>0.05).

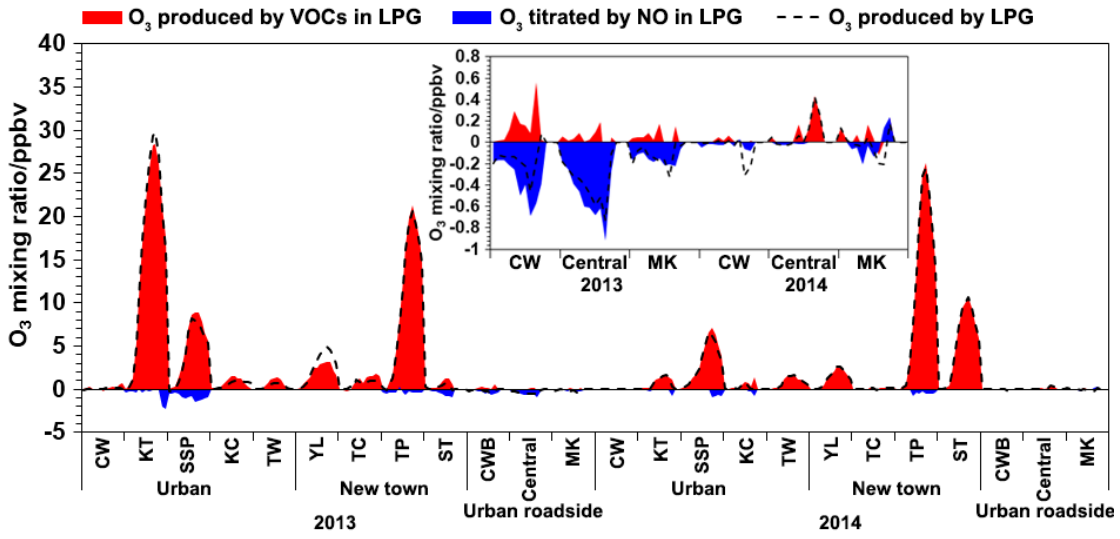

Figure 6 Contribution of LPG vehicle exhaust to O_3 production before and after the program. O_3 production by LPG at the roadside sites is enlarged in the insert panel.

Table 5 Site-dependent average contributions of LPG vehicle exhaust to O_3 production (Unit: ppbv)

	Before	After
Urban roadside	-0.17 ± 0.06	0.004 ± 0.038
Urban	4.19 ± 1.92	0.95 ± 0.38
New town	3.37 ± 1.56	4.47 ± 1.89

3.5 Spatial characteristics of O_3-precursor relationship

Figure 7 shows the relative incremental reactivity (RIR) of anthropogenic VOCs (AHC), biogenic VOCs (BHC), CO and NO_x, as a measure of the sensitivity of O_3 formation to the

changes of the precursors (Cardelino and Chameides, 1995). The VOC groups and CO had positive RIR values, and the RIR values of VOC groups were higher than that of CO, indicating that O_3 production was VOC-limited. The RIR values of AHC were mostly the highest, followed by BHC and CO. In contrast, the average RIR for NO_x was negative, suggesting that cutting NO_x led to O_3 increase. Different from other sites where O_3 formation was limited by AHC, BHC at the rural site TM was the most predominant reagent limiting O_3 formation in September 2013, whereas the RIR of NO_x in September 2014 became positive, same as VOCs and CO, indicating that O_3 formation was limited by both VOCs and NO_x. To understand the dominant VOC groups/species responsible for O_3 formation, Table 6 shows the average RIR values of VOC groups/species at different types of sites (The RIR value of each VOC species is given in Table S4). The alkenes (6.91) and aromatics (7.01) had comparable RIR values and were the highest at the roadside sites, indicating that vehicular emissions were the most important sources of O_3 formation at roadside sites. On the other hand, the aromatics at the urban and new town sites were the most predominant VOCs for O_3 formation, with the RIR values of 20.48 and 24.15, respectively. Solvent usage and traffic emissions were likely the main contributors at these two types of sites. In contrast, isoprene was responsible for O_3 formation at rural site with the RIR of 19.38.

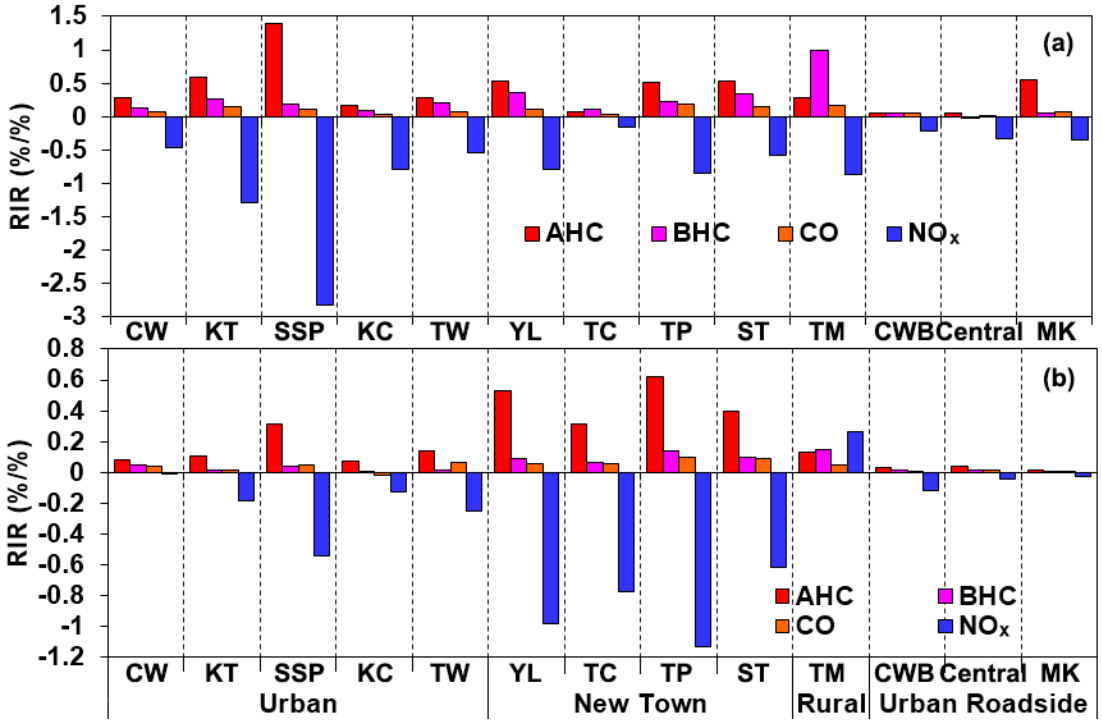

Figure 7 RIR values of VOC groups, CO and NO_x at different sites on (a) 27 Sept. 2013 and (b) 24 Sept. 2014

Table 6 Average RIR of VOC groups or species at different sites (Unit: %/%)

	Urban roadside	Urban	New town	Rural
Alkanes	4.22	8.72	9.67	7.98
Alkenes	**6.91**	10.24	11.35	8.35
Aromatics	**7.01**	**20.48**	**24.15**	15.19
Isoprene	1.31	4.18	8.56	**19.38**
Ethyne	0.02	0.19	0.31	0.81

4 Conclusions

VOC canister samples were collected at 30 sites in Hong Kong before and after the LPG converter replacement program. Source apportionment revealed that the VOCs emitted from LPG-fueled vehicles significantly decreased at urban roadside sites after the program, while they remained unchanged at urban and new town sites. LPG vehicle exhaust was destructive to O_3 formation at the roadside sites before the program, whereas it switched to positive contribution after the program. Nevertheless, the resulting O_3 increase was minor (3.1%). Although the decrease of VOCs and NO in LPG emissions was insignificant at the urban sites, O_3 produced by

LPG vehicle reduced significantly during the program. The above results confirmed the success of the program, particularly in roadside and urban environments. Furthermore, O_3 formation was mainly limited by VOCs regardless of locations, while VOCs and NO_x could co-control the O_3 formation in rural areas. In addition, anthropogenic VOCs were the main species dominating O_3 formation, *i.e.*, alkenes and aromatics in urban roadside environments, and aromatics at urban and new town sites, while O_3 formation at rural sites was most sensitive to biogenic VOCs. The spatial characteristics of O_3-precursor relationships provided useful guideline for the formulation and implementation of O_3 abatement strategies in different-function areas of Hong Kong.

Acknowledgments

We thank HKEPD for providing us the data. This study was supported by the Research Grants Council of the Hong Kong Special Administrative Region via grants (PolyU5154/13E, PolyU152052/14E, CRF/C5022-14G and CRF/C5004-15E), the HKPolyU PhD scholarship (project #RTUP), and the HKPolyU internal grants (1-ZVCX and G-YBHT). This study is partly supported by the National Natural Science Foundation of China (41275122).

References

Alicke B, Geyer A, Hofzumahaus A, Holland F, Konrad S, Pätz HW, et al. OH formation by HONO photolysis during the BERLIOZ experiment. Journal of Geophysical Research-Atmospheres 2003; 108: PHO 3-1-PHO 3-17.

Borbon A, Locoge N, Veillerot M, Galloo JC, Guillermo R. Characterisation of NMHCs in a French urban atmosphere: overview of the main sources. Science of the Total Environment 2002; 292: 177-191.

Cardelino C. Daily Variability of Motor Vehicle Emissions Derived from Traffic Counter Data. Journal of Air & Waste Management Association 1998; 48: 637-645.

Cardelino CA, Chameides WL. An Observation-Based Model for Analyzing Ozone Precursor Relationships in the Urban Atmosphere. Journal of Air & Waste Management Association 1995; 45: 161-180.

406 Censtatd. Census and Statistics Department HKG. Geography and climate, Hong Kong.
407 http://www.censtatd.gov.hk/FileManager/EN/Content_810/geog.pdf retrieved 27 January 2016.
408 Cheng HR, Guo H, Saunders SM, Lam SHM, Jiang F, Wang XM, et al. Assessing photochemical
409 ozone formation in the Pearl River Delta with a photochemical trajectory model. Atmospheric
410 Environment 2010a; 44: 4199-4208.
411 Cheng HR, Guo H, Wang XM, Saunders SM, Lam SHM, Jiang F, et al. On the relationship
412 between ozone and its precursors in the Pearl River Delta: application of an observation-based
413 model (OBM). Environmental Science and Pollution Research 2010b; 17: 547-560.
414 Colman JJ, Swanson AL, Meinardi S, Sive BC, Blake DR, Rowland FS. Description of the
415 Analysis of a Wide Range of Volatile Organic Compounds in Whole Air Samples Collected
416 during PEM-Tropics A and B. Analytical Chemistry 2001; 73: 3723-3731.
417 Creilson JK, Fishman J, Wozniak AE. Intercontinental transport of tropospheric ozone: a study of
418 its seasonal variability across the North Atlantic utilizing tropospheric ozone residuals and its
419 relationship to the North Atlantic Oscillation. Atmospheric Chemistry and Physics 2003; 3:
420 2053-2066.
421 Guenther AB. Modeling biogenic volatile organic compound emissions to the atmosphere. In
422 *Reactive hydrocarbons in the atmosphere*, Nicholas Hewitt editted. Elsevier Inc., London,
423 1999: 98-116.
424 Guenther AB, Zimmerman PR, Harley PC, Monson RK, Fall R. Isoprene and monoterpene
425 emission rate variability: Model evaluations and sensitivity analyses. Journal of Geophysical
426 Research-Atmospheres 1993; 98: 12609-12617.
427 Guo H, Cheng HR, Ling ZH, Louie PKK, Ayoko GA. Which emission sources are responsible
428 for the volatile organic compounds in the atmosphere of Pearl River Delta? Journal of
429 Hazardous Materials 2011a; 188: 116-124.
430 Guo H, So KL, Simpson IJ, Barletta B, Meinardi S, Blake DR. C-1-C-8 volatile organic
431 compounds in the atmosphere of Hong Kong: Overview of atmospheric processing and source

apportionment. Atmospheric Environment 2007; 41: 1456-1472.

Guo H, Wang T, Blake DR, Simpson IJ, Kwok YH, Li YS. Regional and local contributions to ambient non-methane volatile organic compounds at a polluted rural/coastal site in Pearl River Delta, China. Atmospheric Environment 2006; 40: 2345-2359.

Guo H, Zou SC, Tsai WY, Chan LY, Blake DR. Emission characteristics of nonmethane hydrocarbons from private cars and taxis at different driving speeds in Hong Kong. Atmospheric Environment 2011b; 45: 2711-2721.

HKEPD. Characterisation of VOC Sources and Integrated Photochemical Ozone Analysis in Hong Kong and the Pearl River Delta region. Internal Report, 2013.

HKEPD. Pearl River Delta Regional Air Quality Monitoring Network Report http://www.epd.gov.hk/epd/english/resources_pub/publications/m_report.html 2015a.

HKEPD. Hong Kong Air Pollutant Emission Inventory. http://www.epd.gov.hk/epd/english/environmentinhk/air/data/emission_inve.html 2015b.

Ho KF, Lee SC, Ho WK, Blake DR, Cheng Y, Li YS, et al. Vehicular emission of volatile organic compounds (VOCs) from a tunnel study in Hong Kong. Atmospheric Chemistry and Physics 2009; 9: 7491-7504.

Holzworth GC. Mixing Depths, Wind Speeds and Air Pollution Potential for Selected Locations in the United States. Journal of Applied Meteorology 1967; 6: 1039-1044.

Jacobson MZ. Fundamentals of Atmospheric Modelling: Cambridge University Press, 2005.

Jenkin ME, Clemitshaw KC. Ozone and other secondary photochemical pollutants: chemical processes governing their formation in the planetary boundary layer. Atmospheric Environment 2000; 34: 2499-2527.

Kleffmann J, Gavriloaiei T, Hofzumahaus A, Holland F, Koppmann R, Rupp L, et al. Daytime formation of nitrous acid: A major source of OH radicals in a forest. Geophysical Research Letters 2005; 32.

Lam SHM, Saunders SM, Guo H, Ling ZH, Jiang F, Wang XM, et al. Modelling VOC source

458 impacts on high ozone episode days observed at a mountain summit in Hong Kong under the
459 influence of mountain-valley breezes. Atmospheric Environment 2013; 81: 166-176.
460 Lam WHK, Tang YF, Chan KS, Tam ML. Short-term hourly traffic forecasts using Hong Kong
461 Annual Traffic Census. Transportation 2006; 33: 291-310.
462 Lau AKH, Yuan ZB, Yu JZ, Louie PKK. Source apportionment of ambient volatile organic
463 compounds in Hong Kong. Science of the Total Environment 2010; 408: 4138-4149.
464 Li Y, Lau AKH, Fung JCH, Ma H, Tse YY. Systematic evaluation of ozone control policies using
465 an Ozone Source Apportionment method. Atmospheric Environment 2013; 76: 136-146.
466 Li Y, Lau AKH, Fung JCH, Zheng JY, Zhong LJ, Louie PKK. Ozone source apportionment
467 (OSAT) to differentiate local regional and super-regional source contributions in the Pearl
468 River Delta region, China. Journal of Geophysical Research-Atmospheres 2012; 117.
469 Ling ZH, Guo H, Cheng HR, Yu YF. Sources of ambient volatile organic compounds and their
470 contributions to photochemical ozone formation at a site in the Pearl River Delta, southern
471 China. Environmental Pollution 2011; 159: 2310-2319.
472 Ling ZH, Guo H, Lam SHM, Saunders SM, Wang T. Atmospheric photochemical reactivity and
473 ozone production at two sites in Hong Kong: Application of a Master Chemical Mechanism-
474 photochemical box model. Journal of Geophysical Research-Atmospheres 2014; 119.
475 Ling ZH, Guo H, Zheng JY, Louie PKK, Cheng HR, Jiang F, Cheung K, Wong LC, Feng XQ.
476 Establishing a conceptual model for photochemical ozone pollution in subtropical Hong Kong.
477 Atmospheric Environment 2013; 76: 208-220.
478 Louie PKK, Ho JWK, Tsang RCW, Blake DR, Lau AKH, Yu JZ, et al. VOCs and OVOCs
479 distribution and control policy implications in Pearl River Delta region, China. Atmospheric
480 Environment 2013; 76: 125-135.
481 Lu K, Zhang Y. Observations of HOx Radical in Field Studies and the Analysis of Its Chemical
482 Mechanism. Progress in Chemistry 2010; 22: 500-514.
483 Lyu XP, Chen N, Guo H, Zhang WH, Wang N, Wang Y, et al. Ambient volatile organic

484 compounds and their effect on ozone production in Wuhan, central China. Science of the Total
485 Environment 2016; 541: 200-209.
486 Lyu XP, Guo H, Simpson IJ, Meinardi S, Louie PKK, Ling ZH, et al. Effectiveness of replacing
487 catalytic converters in LPG-fueled vehicles in Hong Kong. Atmospheirc Chemistry and
488 Physics Discussion 2015a; 15: 35939-35990.
489 Lyu XP, Ling ZH, Guo H, Saunders SM, Lam SHM, Wang N, et al. Re-examination of C1–C5
490 alkyl nitrates in Hong Kong using an observation-based model. Atmospheric Environment
491 2015b; 120: 28-37.
492 Mao JQ, Ren XR, Chen SA, Brune WH, Chen Z, Martinez M, et al. Atmospheric oxidation
493 capacity in the summer of Houston 2006: Comparison with summer measurements in other
494 metropolitan studies. Atmospheric Environment 2010; 44: 4107-4115.
495 Ou J, Guo H, Zheng J, Cheung K, Louie PKK, Ling Z, et al. Concentrations and sources of non-
496 methane hydrocarbons (NMHCs) from 2005 to 2013 in Hong Kong: A multi-year real-time
497 data analysis. Atmospheric Environment 2015; 103: 196-206.
498 Paatero P. Least squares formulation of robust non-negative factor analysis. Chemometrics and
499 Intelligent Laboratory Systems 1997; 37: 23-35.
500 Paatero P, Tapper U. Positive matrix factorization: A non-negative factor model with optimal
501 utilization of error estimates of data values. Environmetrics 1994; 5: 111-126.
502 Ren X, Brune WH, Oliger A, Metcalf AR, Simpas JB, Shirley T, et al. OH, HO2, and OH
503 reactivity during the PMTACS–NY Whiteface Mountain 2002 campaign: Observations and
504 model comparison. Journal of Geophysical Research-Atmospheres 2006; 111: D10.
505 Ren XR, van Duin D, Cazorla M, Chen S, Mao JQ, Zhang L, et al. Atmospheric oxidation
506 chemistry and ozone production: Results from SHARP 2009 in Houston, Texas. Journal of
507 Geophysical Research-Atmospheres 2013; 118: 5770-5780.
508 Seinfeld JH, Pandis SN. Atmospheric Chemistry and Physics: From Air Pollution to Climate
509 Change. John Wiley & Sons, Inc., 1997.

510 Simpson IJ, Blake NJ, Barletta B, Diskin GS, Fuelberg HE, Gorham K, et al. Characterization of
511 trace gases measured over Alberta oil sands mining operations: 76 speciated C-2-C-10 volatile
512 organic compounds (VOCs), CO2, CH4, CO, NO, NO2, NOy, O3 and SO2. Atmospheric
513 Chemistry and Physics 2010; 10: 11931-11954.
514 Sommariva R, Haggerstone AL, Carpenter LJ, Carslaw N, Creasey DJ, Heard DE, et al. OH and
515 HO2 chemistry in clean marine air during SOAPEX-2. Atmospheric Chemistry and Physics
516 2004; 4: 839-856.
517 USEPA. EPA Positive Matrix Factorization (PMF) 3.0 Fundamentals & User Guide.
518 www.epa.gov 2008.
519 USEPA. User's Guide for the Industrial Source Complex (ISC3) Dispersion Models, Volume II
520 Description of Model Algorithms. EPA-454/B-95-003b. U.S. Environmental Protection
521 Agency, Research Triangle Park, NC. 1985.
522 Wang J-L, Wang C-H, Lai C-H, Chang C-C, Liu Y, Zhang Y, et al. Characterization of ozone
523 precursors in the Pearl River Delta by time series observation of non-methane hydrocarbons.
524 Atmospheric Environment 2008; 42: 6233-6246.
525 Wang T, Wei XL, Ding AJ, Poon CN, Lam KS, Li YS, et al. Increasing surface ozone
526 concentrations in the background atmosphere of Southern China, 1994–2007. Atmospheric
527 Chemistr and Physics 2009; 9: 6217-6227.
528 WebMET. Met Monitoring Guide, The Meteorological Resource Center.
529 http://www.webmet.com/met_monitoring/622.html accessed on 30 July 2015 2015; 6.2.2
530 Vector computations.
531 Xia L, Shao Y. Modelling of traffic flow and air pollution emission with application to Hong
532 Kong Island. Environmental Modelling & Software 2005; 20: 1175-1188.
533 Xue LK, Wang T, Guo H, Blake DR, Tang J, Zhang XC, et al. Sources and photochemistry of
534 volatile organic compounds in the remote atmosphere of western China: results from the Mt.
535 Waliguan Observatory. Atmospheric Chemistry and Physics 2013; 13: 8551-8567.

536 Xue LK, Wang T, Louie PKK, Luk CWY, Blake DR, Xu Z. Increasing External Effects Negate
537 Local Efforts to Control Ozone Air Pollution: A Case Study of Hong Kong and Implications
538 for Other Chinese Cities. Environmental Science & Technology 2014; 48: 10769-10775.
539 Xue LK, Wang T, Zhang JM, Zhang XC, Deliger, Poon CN, et al. Source of surface ozone and
540 reactive nitrogen speciation at Mount Waliguan in western China: New insights from the 2006
541 summer study. Journal of Geophysical Research-Atmospheres 2011; 116: D07306.
542 Zhang J, Wang T, Chameides WL, Cardelino C, Kwok J, Blake DR, et al. Ozone production and
543 hydrocarbon reactivity in Hong Kong, Southern China. Atmospheric Chemistry and Physics
544 2007; 7: 557-573.

Spatiotemporal variation of ozone precursors and ozone formation in Hong Kong: Grid field measurement and modelling study

X.P. Lyu[1], M. Liu[1], H. Guo*[1], Z.H. Ling[1], Y. Wang[1], P.K.K. Louie[2], C.W.Y. Luk[2]

1. *Air Quality Studies, Department of Civil and Environmental Engineering, The Hong Kong Polytechnic University, Hong Kong*
2. *Air Group, Hong Kong Environmental Protection Department, Hong Kong*

*Corresponding author. ceguohai@polyu.edu.hk

Abstract

Grid field measurements of volatile organic compounds (VOCs) covering the entire territory of Hong Kong were simultaneously carried out twice daily on 27 September 2013 and 24 September 2014, respectively, to advance our understanding on the spatiotemporal variations of VOCs and ozone (O_3) formation, the factors controlling O_3 formation and the efficacy of a control measure in Hong Kong. From before to after the control measure on liquefied petroleum gas (LPG) fueled vehicles, the VOCs originated from LPG vehicle exhaust deceased from 41.3 ± 1.2 μg/m^3 (49.7±1.5%) to 32.8±1.4 μg/m^3 (38.8±1.7%) (p<0.05). In contrast, the contribution to VOCs made by gasoline and diesel vehicle exhaust and solvent usage increased (p<0.05). VOCs and nitric oxide (NO) in LPG source experienced the highest reductions at the roadside sites, while the variations were not significant at the urban and new town sites (p>0.05). For O_3 production, LPG vehicle exhaust generally made a negative contribution (-0.17±0.06 ppbv) at the roadside sites, however it turned to a slightly positive contribution (0.004 ± 0.038 ppbv) after the control measure. At the urban sites, although the reduction of VOCs and NO was minor (p>0.05), O_3 produced by LPG vehicle significantly reduced from 4.19±1.92 ppbv to 0.95±0.38 ppbv (p<0.05). Meanwhile, O_3 produced by LPG at the new town sites remained stable. The analysis of O_3-precursor relationships revealed that alkenes and aromatics were the main species limiting roadside O_3 formation, while aromatics were the most predominant controlling factor at urban and new town sites. In contrast, isoprene and sometimes NO_x limited the O_3 formation in rural environment.

Keywords: VOCs; source apportionment; photochemical O_3; Eulerian box model; MCM

1 Introduction

Well known as a major air pollutant in the atmosphere, ozone (O_3) has attracted increasing concerns in recent years due to its adverse effects on human health, visibility and ecosystem (Louie et al., 2013; Wang et al., 2008). O_3 is formed by a series of complex photochemical reactions involving volatile organic compounds (VOCs) and nitrogen oxides (NO_x) in the presence of sunlight (Seinfeld and Pandis, 1997). Since photochemical O_3 formation has a nonlinear relationship with its precursors, *i.e.*, VOCs and NO_x, it is difficult to remediate the photochemical pollution, especially in the regions with frequently high O_3 events, such as the Pearl River Delta (PRD).

Continuously rapid urbanization and population growth in Hong Kong coupled with high surface VOCs and NO_x emission, high solar radiation and hot weather make this region a photochemically polluted area. Previous studies have reported that the photochemical O_3 formation in Hong Kong is generally VOC-limited (Cheng et al., 2010a, b; Zhang et al., 2007). Furthermore, a number of studies were carried out on the contributions to O_3 in Hong Kong of regional transport from PRD and superregional transport from eastern China (Xue et al., 2014; Li et al., 2012, 2013; Ling et al., 2013; Wang et al., 2009), and several efforts have been made to study formation mechanism of O_3 pollution in Hong Kong (Ling et al., 2014; Xue et al., 2014). Although Ling et al. (2014) revealed that photochemical reactivity and ozone production were absolutely different between a semirural site and an urban site in Hong Kong, there is little knowledge about the spatial patterns of the relationship between O_3 and its precursors.

In addition, a series of control measures have been implemented in Hong Kong to reduce VOCs emitted from different anthropogenic sources, including VOC-containing products, road transport and industry emissions to mitigate O_3 pollution (HKEPD, 2015a; Louie et al., 2013). Hence, grid field measurements pre- and post- a control measure would help assess the effectiveness of the measure. For example, promotion of LPG as a substitute fuel for taxi and public light buses in Hong Kong was the most striking measure to reduce VOC emissions in the

past decade. However, recently, LPG usage was found to become major contributor to ambient VOCs in Hong Kong due to poor maintenance (Lau et al., 2010; Ling et al., 2014). In general, the catalytic converters in the LPG-fueled vehicles should be replaced every 1-2 years, depending on maintenance and mileage. In Hong Kong, about 80% of taxis and 45% of public light buses using LPG as fuel have defective converters, resulting in excessive emissions of vehicle exhaust (HKEPD, 2013). As such, to reduce LPG-fueled vehicle emissions, the Hong Kong government set aside $150 million to replace the catalytic converters and associated components on LPG-fueled taxis and public light buses, which commenced in October 2013 and completed in April 2014. It is well known that properly functioning catalytic converters in the LPG-fueled vehicles could reduce emissions up to 90%.

Therefore, the objectives of this study were to evaluate the benefit of replacing catalytic converters and oxygen sensors on LPG-fueled vehicles, to examine the spatiotemporal variations of O_3 production by LPG, and to study the spatial characteristics of O_3-precursor relationships in Hong Kong.

2 Methodology

2.1 Grid sampling campaigns

Totally 30 sampling sites were selected in different districts covering the entire territory of Hong Kong. The grid measurement campaigns were conducted on 27 September 2013 and 24 September 2014, respectively. At each of the 30 sites, 3-minute VOC canister samples were collected once in the morning between 9:00 and 11:00 and another in the afternoon between 2:00 and 4:00. Two of the 30 sites had duplicate samples. In total, 64 samples were collected for each campaign. The 30 sites included 24 roadside sites and 6 general sites (Figure 1 and Table S1).

Thirteen out of the 30 sites were the Hong Kong Air Quality Monitoring Stations (AQMS) (http://epic.epd.gov.hk/EPICDI/air/station/) (Table 1), where trace gas data were available. These sites covered the entire territory of Hong Kong and could provide a full picture of photochemical O_3 formation. The 13 AQMSs were categorized into four types according to the land usage and

the distance from urban center, *i.e.*, 3 urban roadside sites, 5 urban sites, 4 new town sites and 1 rural site (Figure 1 and Table 1).

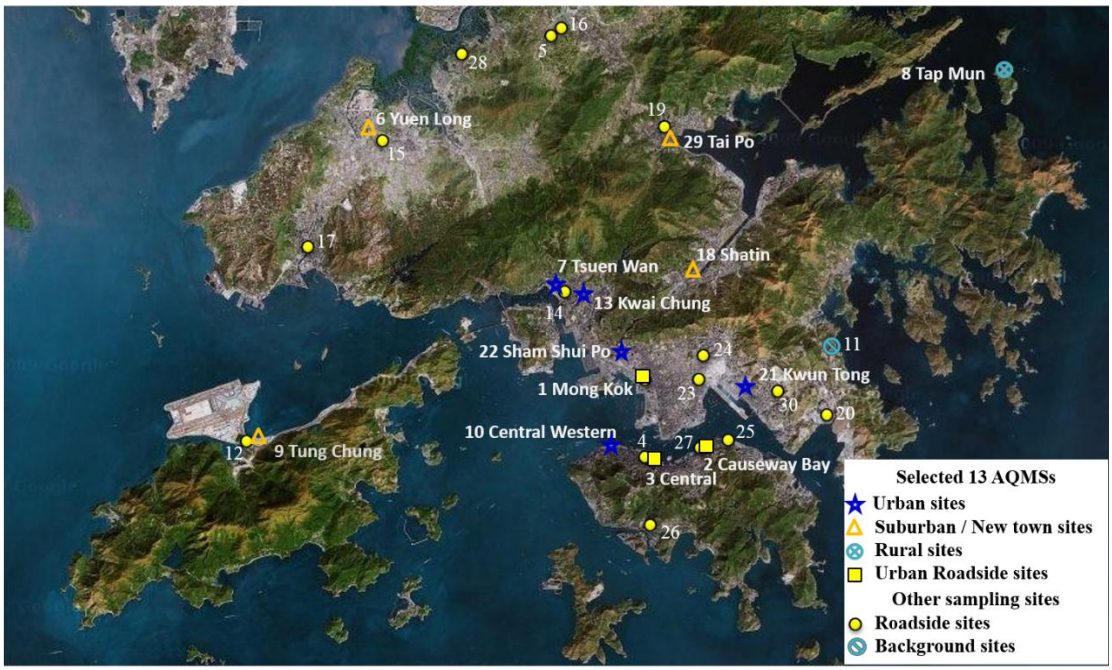

Figure 1 Geographic location of the sampling sites and surrounding environments.

Table 1 Description of the 13 AQMS sites

Type	Site	No.*	Description
Urban	Central Western (CW)	10	General urban air quality monitoring stations in residential areas and some mixed with commercial and/or industrial areas.
	Kwun Tong (KT)	21	
	Sham Shui Po (SSP)	22	
	Kwai Chung (KC)	13	
	Tsuen Wan (TW)	7	
Suburban/ New Town	Yuen Long (YL)	6	Mainly residential areas in new territories.
	Tung Chung (TC)	9	
	Tai Po (TP)	29	
	Sha Tin (ST)	18	
Rural	Tap Mun (TM)	8	Remote island off the northeast coast of Hong Kong
Roadside	Causeway Bay (CWB)	2	Commercial centers with high-rise buildings along the streets, high traffic and pedestrian flow, and frequent traffic jam in
	Central	3	

	Mong Kok (MK)	1	rush hours

* Sequence number in Figure 1.

2.2 Collection and analysis of VOC samples

Ambient VOC samples were collected using cleaned and evacuated 2 L electro-polished stainless steel canisters. The canisters were prepared and delivered to Hong Kong by the Rowland/Blake group at University of California, Irvine (UCI). A flow-controlling device was used to collect the samples for 3 minutes.

Before sampling, all canisters were cleaned at least five times by repeatedly filling and evacuating with humidified pure nitrogen gas (N_2). To test for any contamination in the canister, the evacuated canister was filled with pure N_2, stored for at least 24 h, then checked by the same VOC analytical methods to ensure that all the target compounds were not found or were under the method detection limit (MDL). In addition, duplicate samples were regularly collected to check the precision and reliability of the sampling and analytical methods. After sampling, the VOC samples were returned to the laboratory at UCI for chemical analysis. The analytical system, which was fully described in Simpson et al. (2010), used multicolumn gas chromatography (GC) with five column-detector combinations. The oven parameters employed for each GC can be found in Colman et al. (2001). In total, 39 non-methane hydrocarbons (NMHCs), methane (CH_4) and carbon monoxide (CO) were quantified from the canister samples. VOCs were identified via their retention time and mass spectra. The quantification of target VOCs was accomplished using multipoint external calibration curves, obtained from a combination of National Bureau of Standards, Scott Specialty Gases (absolute accuracy estimated to be within ±5 %) and UCI made standards. The detection limit, measurement precision and accuracy for each VOC varied and were listed in Simpson et al. (2010). Generally, alkanes, alkenes and aromatics had a detection limit of 3 pptv, a precision of 3%, and an accuracy of 5%.

For on-line measurements of VOCs, which were mainly used in section 2.5, a built-in computerized program, including auto-linearization, auto-calibration and calibration with span gas, was adopted to control the quality. The accuracy and precision of VOC measurements were 1.0-10.0% and 2.5-20.0 %, respectively.

2.3 PMF model

US EPA PMF model (version 5.0) was applied to the measurement data for receptor-based source appointment. The PMF model is a multivariate factor analysis tool that decomposes a matrix of speciated sample data into two matrices - factor contributions and factor profiles which can be interpreted by an analyst as to what sources are represented based on observations at the receptor site (Paatero, 1997; Paatero and Tapper, 1994).

The details of PMF applied to VOC data for source profiles and the contributions of individual VOC species have been introduced somewhere else (Guo et al., 2011a; Ling et al., 2011; Ou et al., 2015). Briefly, 18 NMHCs were input into the PMF model and the uncertainties for each sample/species were determined as the sum of 5-15% of VOC concentration and two times the method detection limit (MDL) of the species (USEPA, 2008). Values below the MDL were replaced by half of the MDL values and their overall uncertainties were set as 5/6 of the MDL values. Results were constrained so that no samples had negative source contributions. Different number of factors and uncertainties were tested, and an optimum solution was determined based on a good fit to the observed data and the most meaningful results by comparing with previous studies (Guo et al., 2011a, b; Lau et al., 2010).

2.4 Calculation of VOCs diurnal profiles

Since VOCs canister samples at the 30 sites were only collected at ~10:00 and 15:00, respectively, it was impossible to use them for a photochemical box modeling as the model required hourly data input for consecutive hours. Hence, it is necessary to derive time-dependent concentrations from the two canister samples for the use in the photochemical box model incorporating master chemical mechanism (PBM-MCM). The procedures to obtain hourly VOC

profiles from two samples were similar to the method described in Zhang et al. (2007). Briefly, the method was based on the mass conservation of a species inside a fixed Eulerian box, namely, the Eulerian box model (Seinfeld and Pandis, 1997). The entraining equations are:

$$\frac{dC_i}{dt} = \frac{q_i}{H(t)} + R_i - \frac{v_{d,i}}{H(t)} C_i + \frac{C_i^0 - C_i}{\tau_\gamma} \quad \text{for} \quad \frac{dH}{dt} \le 0 \qquad (1)$$

$$\frac{dC_i}{dt} = \frac{q_i}{H(t)} + R_i - \frac{v_{d,i}}{H(t)} C_i + \frac{C_i^0 - C_i}{\tau_\gamma} + \frac{C_i^a - C_i}{H(t)} \frac{dH}{dt} \quad \text{for} \quad \frac{dH}{dt} > 0 \qquad (2)$$

where, C_i: Concentration of species i (μg m^{-3}),

q_i : Emission rate of species i (μg m^{-2} s^{-1}),

$H(t)$: Mixing height as a function of time t (m),

R_i: Chemical destruction rate of species i (μg m^{-3} s^{-1}),

$\upsilon_{d,i}$: Dry/wet deposition rate of species i (m s^{-1}),

C_i^0: Background concentration of species i (μg m^{-3}),

τ_γ: Residence time of air over the area (s),

C_i^a: Concentration of species i above the boundary layer (μg m^{-3}).

Equations (1) and (2) mathematically describe the concentration of species above a given area, assuming that the corresponding airshed is well mixed, accounting for emissions, chemical reactions, removal, advection of material in and out of the airshed, and entrainment of material during growth of the mixing layer. Before the numerical solutions of equations (1) and (2) are solved with Gear's backward differentiation formula (Jacobson, 2005), the parameters in equations (1) and (2) need to be determined.

Emission Rates: the Hong Kong emission inventory of total anthropogenic VOCs from different sources in 2013 was used to estimate the annual emission amount (HKEPD, 2015b). This annual emission amount was then equally allocated to 52 weeks and the area of 1104 square kilometers covering Hong Kong territory. The area of Hong Kong was obtained from Censtatd (2016), while the days were classified as weekdays and weekends, and the emission factors of each day of a

week were determined by Cardelino (1998). Hence, the daily initial emission amount of total VOCs per unit area was calculated. This value was multiplied by the typical profile of ambient VOCs, which was obtained by averaging all canister data at different sites, to derive the daily initial emission rates of speciated VOCs at different sites. The diurnal variations of the anthropogenic VOC emissions were estimated according to source types. Industry and power generation were assumed to have no diurnal variations, while mobile emission had the same pattern as traffic flow in Hong Kong (Lam et al., 2006; Xia and Shao, 2005). The diurnal variation of biogenic VOCs (*i.e.*, isoprene) was estimated by considering the temperature variations and the best fit value coefficient T_M, which affected the predicted emission behavior at high temperatures (Guenther, 1993, 1999). In this way, the speciated VOCs emission rates from different sources were determined.

Mixing Height Profile: The mixing height was estimated using the Holzworth method (Holzworth, 1967). The Holzworth method provides twice-per-day (morning and afternoon) mixing heights based on calculations using routine upper-air data and minimum and maximum temperature of the day. The upper air sounding data were obtained from the University of Wyoming (http://weather.uwyo.edu/upperair/sounding.html). The minimum temperature was determined from the data of King's Park station operated by Hong Kong Observatory (HKO) (http://www.hko.gov.hk/) for the time period of 0200-0600 local standard time (LST). Here, we followed the method of Zhang et al. (2007), which also calculated the mixing height in Hong Kong by using "plus 2 °C" to the morning minimum surface temperature to calculate the morning mixing height. The afternoon mixing height was calculated using the maximum surface temperature observed at 1200-1600. The hourly mixing heights, often used in regulatory dispersion modeling, were interpolated from these twice-per-day estimates. The recommended interpolation procedure is provided in the user's guide for the Industrial Source Complex (ISC) dispersion model (USEPA, 1985).

The dry/wet deposition rate and the concentration above the boundary layer were assumed to be

zero for all VOCs. Background concentrations of VOCs were expressed as geometric mean concentrations at general sites. Residence time of air over the area was the ratio of length of the box to wind speed, and the time-dependent wind speed was determined by curve fitting using the in-situ hourly wind speed obtained from the HKO. Since length of the box and emission rates of VOCs at different sites were different and the VOC chemical destruction rates were unknown, we adopted an iterative approach to determine these parameters based on canister data at 10:00 and 15:00. We first used a typical OH profile in clean marine atmosphere (Creasey et al., 2003) and the initial emission rate of propane to calculate the temporal variations of propane from 10:00 to 15:00 with the box length ranging from 0 to 60 km (*i.e.*, beyond the longest range of Hong Kong territory). Propane was selected due to its high concentration and lower reactivity with OH compared to alkenes. The optimal emission rate and the length of box were adjusted by matching the calculated propane level at 15:00 with the observed value, using a 5% agreement for consistency. The ratio of optimal emission rate to initial emission rate of propane was defined as emission rate factor. The temporal variation of more reactive propene from 10:00 to 15:00 was calculated in the same way, but the length of box was fixed and the emission rate of propene was modified by multiplying the initial emission rate of propene by the emission rate factor determined by propane above. As such, the original OH profile used above was refined to fit the real situation in Hong Kong. The refined OH profile was then used to recalculate the temporal variation of propane. The entire procedure was called iteration. Iterations were repeated until convergence was obtained. Thus the length of box, emission rates of VOCs and OH profiles at different sites were obtained via this iterative approach.

2.5 PBM-MCM model

The photochemical box model (PBM) incorporating Master Chemical Mechanism (MCM) is a near-explicit chemical mechanism which describes the detailed gas-phase chemical processes involving the tropospheric degradation of a series of primary VOCs. The chemical mechanistic information was extracted from the Master Chemical Mechanism, MCM v3.2 (Jenkin et al., 1997;

Saunders et al., 2003), via website http://mcm.leeds.ac.uk/MCM.

The model was constructed with measured CO, NO, NO_2, SO_2, C_2-C_9 NMHCs, temperature and relative humidity. Data were read every hour to calculate the in-situ rates of O_3 production and destruction. The model has been widely used in Hong Kong (Ling et al., 2014; Lyu et al., 2015b, 2016).

3 Results and discussion

3.1 Meteorological conditions

Figure 2 shows the average geopotential height (HGT) and wind field on 1000 hPa for East Asia during the two sampling campaigns. The pressure (represented with HGT) over Hong Kong was comparable between the two campaigns. The wind was northeasterly on 27 September 2013, while it was calm on 24 September 2014 in Hong Kong. The lower wind speed in the latter campaign was expected to elevate the VOC concentrations. However, the levels of most VOCs remained similar, whereas those emitted from LPG source decreased between the two campaigns (see sections 3.2 and 3.3), indicating that meteorological parameters did not have substantial influence on the VOC levels of the two campaigns.

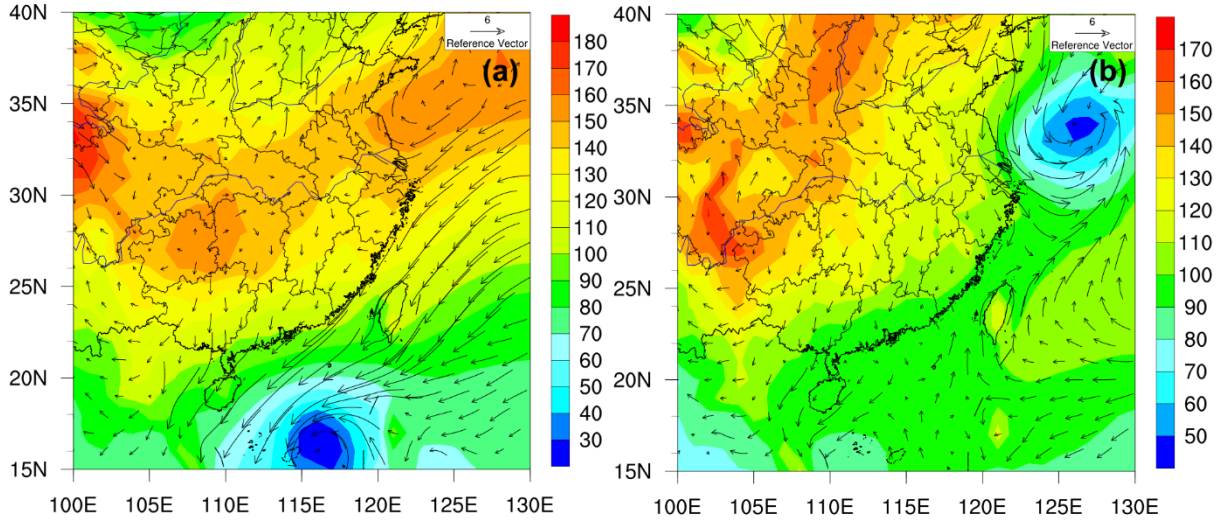

Figure 2 Average geopotential height and wind field on (a) 27 September 2013 and (b) 24 September 2014. The figures are made using NCEP FNL (final) data with a horizontal resolution of 1°×1°.

3.2 Comparison of VOCs between the two campaigns

Table 2 presents the average mixing ratios of VOCs at the 24 roadside sites and 6 general sites during the two campaigns. It is noteworthy that the average VOC values for the sites should reflect the real situation though uncertainties could exist for the samples at individual sites. It was found that the alkanes dominated the total VOC composition, followed by aromatics and alkenes, and the mixing ratios at roadside sites were much higher than those at general sites due to their proximity to the emission sources (p<0.05). From September 2013 to September 2014, values of most species remained unchanged except for *n*/*i*-pentanes, which increased at the general sites (p<0.05), indicating possibly increased emission of gasoline-fueled vehicles. Furthermore, aromatics such as xylenes and propylbenzenes increased significantly (p<0.05), perhaps due to the increase of solvent usage and/or vehicular emissions. In contrast, LPG related VOCs (propane and *n*/*i*-butanes) remained unchanged, while propene, the tracer of LPG combustion, even decreased at the roadside sites (p<0.05). In view of the above fact, to examine whether the replacement program was actually effective, it is necessary to conduct source apportionments to obtain the emission variations of LPG-fueled vehicles before and during the replacement program.

Table 2 Mixing ratio of VOCs collected at the 30 sampling sites during the 2 sampling campaigns (average±95% confidence interval, pptv)

	Species	Roadside sites (n=24) [a]		General sites (n=6) [a]	
		Sept. 2013	Sept. 2014	Sept. 2013	Sept. 2014
Alkanes	Ethane	2518±209	2704±206	1833±179	1884±280
	Propane	7723±1872	6996±1039	3631±2478	2849±1076
	n-Butane	11166±3104	9003±1645	2828±1876	2694±1247
	i-Butane	6413±1726	5455±931	1866±1227	1762±799
	n-Pentane	773±197	1209±457	331±74	866±321 *
	i-Pentane	1331±324	2097±1127	608±112	1372±499 *
	n-Hexane	323±92	529±86 *	148±42	415±177 *
	2,3-Dimethylbutane	118±46	186±51	48±22	137±58 *
	2-Methylpentane	593±193	847±223	301±137	754±408
	3-Methylpentane	315±95	588±153 *	174±85	552±285 *
	n-Heptane	437±242	480±122	122±35	226±93 *
	2-Methylhexane	444±235	416±82	151±51	255±123

	3-Methylhexane	449±243	510±90	145±51	353±156 *
	n-Octane	106±37	137±46	47±10	74±24
	2,2,4-Trimethylpentane	255±132	316±81	37±8	109±66 *
Alkenes	Ethene	4631±917	3748±669	1097±327	1082±398
	Propene	1798±417 *	1084±230	233±70	201±93
	1-Butene	197±40	161±32	53±21	48±25
	i-Butene	566±145 *	371±87	150±58	94±33
	trans-2-Butene	132±36	99±26	20±8	21±8
	cis-2-Butene	82±25	56±15	14±4	13±5
	1-Pentene	55±11	93±49	19±6	28±11
	1,3-Butadiene	149±37	119±24	29±5	17±10
	Isoprene	531±90	627±115	500±230	777±285
Alkyne	Ethyne	3916±671	3375±391	1978±426	2037±404
Aromatics	Benzene	886±138 *	662±64	556±67	518±105
	Toluene	3270±1751	3371±527	1634±610	2745±1136
	Ethylbenzene	643±127	674±87	438±150	703±230
	p-Xylene	291±85	420±69 *	130±39	378±163 *
	m-Xylene	483±178	703±153	161±50	602±296 *
	o-Xylene	337±103	471±79	142±44	428±180 *
	i-Propylbenzene	39±13	42±6	17±4	34±10 *
	n-Propylbenzene	92±39	79±14	30±9	53±16 *
	3-Ethyltoluene	380±210	212±59	66±23	113±47
	4-Ethyltoluene	187±112	119±28	37±10	75±30 *
	2-Ethyltoluene	164±76	87±22	41±12	53±22
	1,3,5-TMB	234±127 *	78±24	40±14	37±15
	1,2,4-TMB	821±486 *	288±85	128±54	145±67
	1,2,3-TMB	228±102	84±22	56±24	45±19

[a] Number of sites; * higher mixing ratios as compared to those in another sampling campaign at the confidence level of 95% (p<0.05). TMB refers to the trimethylbenzene isomers hereafter.

3.3 Source apportionments of VOCs and trace gases

Twenty main anthropogenic VOC species quantified in the 64 samples were applied to PMF for source apportionment for the two campaigns, respectively. The source profiles before and after the intervention program are similar (Figure 3). Three factors were extracted from the PMF model simulation. Since most of the samples were collected at roadside sites, it is expected that vehicular emissions were the dominant sources of VOCs in this study. The first factor was distinguished by the dominance of propane, *n*/*i*-butanes, ethene and propene, representing LPG-fueled vehicle exhaust. Factor 2 had high percentages of all VOCs and trace gases except LPG related component and the trimethylbenzene isomers. It was assigned as gasoline and diesel vehicle exhaust. The third factor was closely associated with solvent usage because of high

loadings of xylenes and trimethylbenzenes. The profiles of factors identified were based on the results of previous source apportionment studies (Guo et al., 2007, 2011a; Lau et al., 2010; Ling et al., 2011) and VOCs source emission studies (Borbon et al., 2002; Guo et al., 2006, 2011b; Ho et al., 2009). Many different starting seeds were tested and no multiple solutions were found. In addition, good correlations were found between the observed and predicted VOC concentrations for the whole dataset (R^2 = 0.95 and 0.96, respectively) before and after the replacement program. Moreover, all of the selected species had scale residuals normally distributed between -3 and 3, confirming that the measured data were well reproduced (USEPA, 2008).

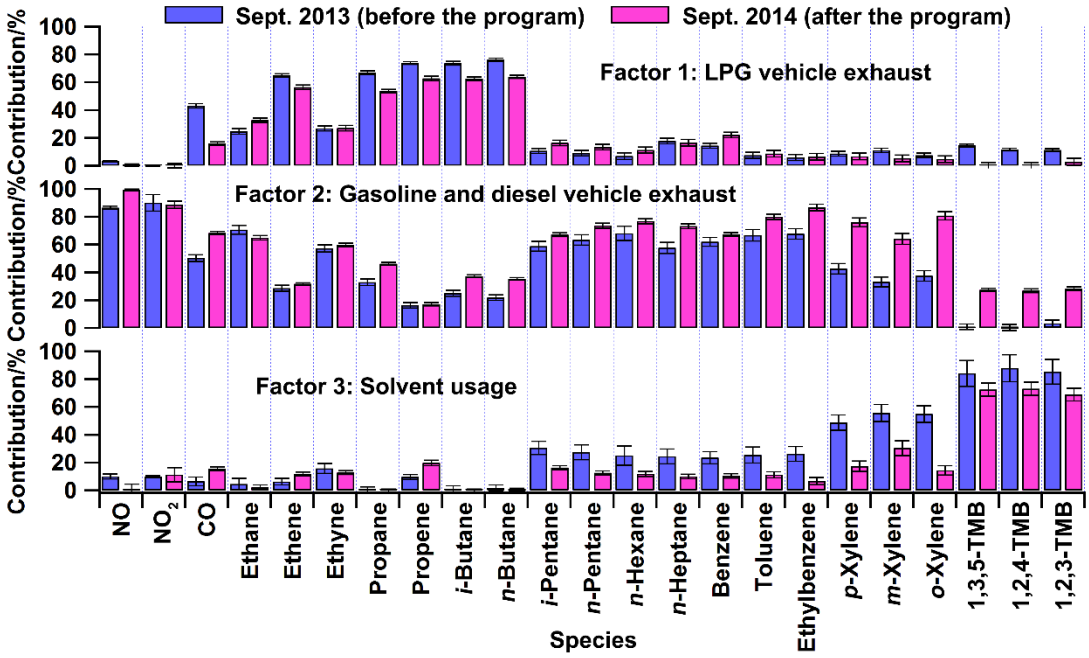

Figure 3 Source profiles of the three sources extracted from PMF in September 2013 (before the program) and September 2014 (after the program). The standard errors are estimated with the bootstrap in the PMF model.

To sum up the VOC concentrations in each source, the mass and percentage contributions of the sources to VOCs are summarized in Table S2. Noticeably, the vehicle emissions were the dominant source of VOCs, with the contribution of 71.1±1.8 μg/m^3 (85.5±2.1%) and 77.7±1.3 μg/m^3 (92.0±1.6%) before and after the program, respectively. From 2013 to 2014, the VOCs emitted from gasoline and diesel vehicles increased remarkably (p<0.05), whereas those

originated from LPG vehicle exhaust decreased significantly (p<0.05) from 41.3±1.2 μg/m^3 (49.7±1.5%) to 32.8±1.4 μg/m^3 (38.8±1.7%). Table 3 shows the average concentrations of VOCs and trace gases in LPG vehicle exhaust. Clearly, CO, ethene, propane, propene, *n*/*i*-butanes and trimethylbenzene isomers all reduced significantly from before to after the replacement program (p<0.05). The emissions of NO and NO_2 from LPG-fueled vehicles were minor, and the decrease of NO was insignificant (p>0.05). Table 4 presents the reductions of VOCs and NO at different sites. The mass and percentage contribution of LPG vehicle exhaust to VOCs experienced the greatest decrease at the roadside sites (p<0.05), with the contributions of 54.7±23.2 μg/m^3 (54.6±10.0%) before and 25.0±11.2 μg/m^3 (30.8±9.9%) after the program, respectively. The effects were much weaker at the urban and new town sites, where the mass and percentage contribution to VOCs decreased slightly or even increased (p>0.05). Similarly, NO decreased noticeably (p<0.05) (before: 0.66±0.28 μg/m^3; after: 0.04±0.02μg/m^3) at roadside sites, while the reductions were not significant at the urban and new town sites (p>0.05). This inter-site difference was possibly caused by higher traffic flow and more dense LPG-fueled vehicles (particularly taxis) in the vehicle fleet at roadside sites.

Table 3 Concentrations of VOCs and trace gases emitted from LPG-fueled vehicles (μg/m^3)

Species	LPG vehicle exhaust	
	before	after
NO	0.49 ± 0.44	0.03 ± 0.44
NO_2	0.00 ± 0.94	0.00 ± 1.05
CO	**336.24 ± 12.71**	**149.5 ± 11.1**
Ethane	0.71 ± 0.06	1.03 ± 0.05
Ethene	**2.83 ± 0.05**	**2.00 ± 0.05**
Ethyne	0.89 ± 0.06	0.87 ± 0.07
Propane	**7.63 ± 0.16**	**6.07 ± 0.14**
Propene	**1.76 ± 0.02**	**0.91 ± 0.02**
***i*-Butane**	**8.93 ± 0.16**	**6.98 ± 0.13**
***n*-Butane**	**16.00 ± 0.26**	**11.52 ± 0.20**
i-Pentane	0.30 ± 0.05	0.75 ± 0.09
n-Pentane	0.14 ± 0.03	0.38 ± 0.06
n-Hexane	0.05 ± 0.02	0.17 ± 0.03
n-Heptane	0.14 ± 0.01	0.20 ± 0.03
Benzene	0.37 ± 0.05	0.44 ± 0.04
Toluene	0.56 ± 0.16	0.94 ± 0.25
Ethylbenzene	0.13 ± 0.05	0.17 ± 0.06

p-Xylene	0.08 ± 0.02	0.10 ± 0.04
m-Xylene	0.14 ± 0.02	0.11 ± 0.05
o-Xylene	0.08 ± 0.02	0.08 ± 0.04
1,3,5-TMB	**0.12 ± 0.01**	**0.00 ± 0.01**
1,2,4-TMB	**0.32 ± 0.03**	**0.00 ± 0.03**
1,2,3-TMB	**0.11 ± 0.01**	**0.01 ± 0.01**

Bolded are the species with significant reduction in LPG vehicle exhaust (p<0.05).

Table 4 Mass and percentage contribution of LPG vehicle exhaust to VOCs and NO at different sites before and after the program

Species	Site	Mass concentration (μg/m^3)		Percentage contribution (%)	
		before	after	before	after
VOCs	Urban roadside	54.7 ± 23.2	25.0 ± 11.2	54.6 ± 10.0	30.8 ± 9.9
	Urban	28.7 ± 35.8	23.7 ± 11.8	29.3 ± 30.3	31.1 ± 10.5
	New town	11.5 ± 9.8	16.5 ± 17.1	27.9 ± 23.6	20.8 ± 20.3
NO	Urban roadside	0.66 ± 0.28	0.02 ± 0.01	0.04 ± 0.02	0.005±0.002
	Urban	0.34 ± 0.42	0.02 ± 0.02	0.03 ± 0.03	0.005±0.004
	New town	0.14 ± 0.12	0.02 ± 0.02	0.01 ± 0.01	0.003±0.004

3.4 Impact of replacement program on O_3 formation

3.4.1 Model validation and O_3 simulation

Since the estimated diurnal profiles of VOCs were used to simulate O_3, it is necessary to validate the results with the online measured VOCs. Figure 4 shows the estimated and online measured diurnal patterns of total VOCs at MK, YL and TC, where the real-time VOCs data were available. 26 VOC species were included in the total VOCs for calculation. The diurnal patterns of total VOCs estimated from the two points of canister sample data agreed well with the real-time measurements. Table S3 lists the Index of Agreement (IOA) values between the calculated and measured data of the 26 VOC species. Within the range of 0~1, higher IOA value indicates better agreement (Wang et al., 2015; Jiang et al., 2010). Fair to good agreement between the calculated and measured profiles of individual VOCs at these three types of sites suggested that the proposed method provided a reasonable estimate of VOC profiles based on the two canister samples. It is noteworthy that the measured and estimated VOC profiles during 01:00-09:00 did not fit very well at MK, probably due to the fact that the concentrations of VOCs, on one hand, were significantly influenced by in-situ traffic emissions as MK was a roadside site. On the other

hand, the method for estimating VOC diurnal profiles in this study was based on emission inventory, which was an averaged profile. This discrepancy in early morning would not substantially influence the simulation of O_3 formation, because O_3 formation was mainly simulated at daytime hours (*i.e.*, 07:00~19:00), and the photochemical reactions of VOCs were weak between 01:00 and 09:00.

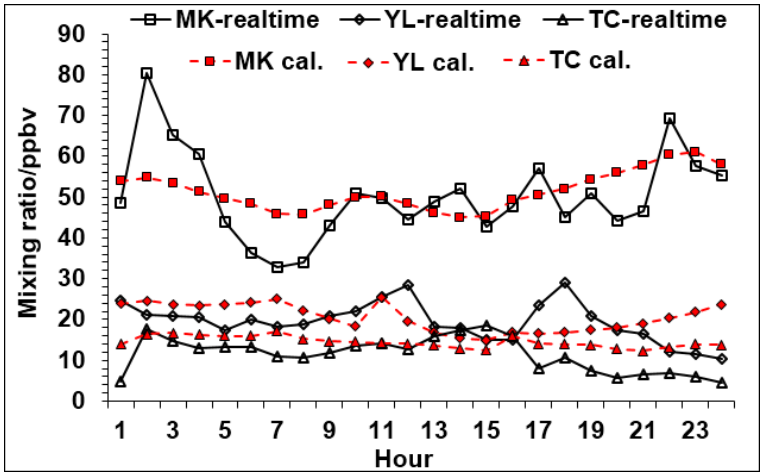

Figure 4 Estimated and real-time measured diurnal profiles of total VOCs at MK, YL and TC.

The calculated VOC diurnal profiles were then input into the PBM-MCM model for O_3 simulation. Figure 5 shows the daytime (07:00~19:00) simulated and observed O_3 in 2013 and 2014 at 13 sites where the online data of trace gases were available from the air quality monitoring network of HKEPD. In general, the simulated O_3 agreed well with the observations, with the consistence of the peaks and troughs. The IOA between the simulated and observed O_3 was 0.7, indicating fairly acceptable performance of the model. In other words, in-situ O_3 formation dominated its ambient level at most sites. The difference between model simulation and observation at some other sites was likely due to the fact that the PBM-MCM model only considers O_3 produced from photochemical reactions while the observed O_3 is also influenced by the downward transport of stratospheric O_3, dry deposition and horizontal transport from other regions/locations (Cheng et al., 2010a; Creilson et al., 2003; Lam et al., 2013; Xue et al., 2011).

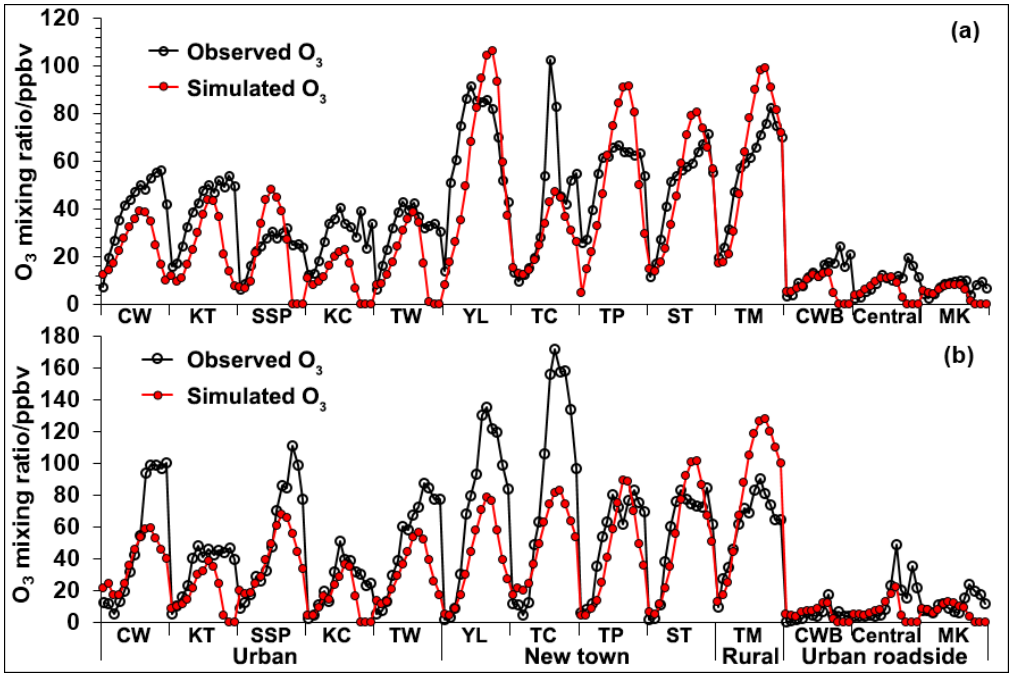

Figure 5 Comparison between simulated and observed O_3 in (a) September 2013 and (b) September 2014.

3.4.2 Impact of the program on O_3 formation

Given the reduction of VOCs and NO emitted from LPG-fueled vehicles, it is interesting to explore the impact of these changes on O_3 formation at different sites.

Sensitivity experiments give the differences in O_3 production between the scenarios with and without the LPG source as input. Through this approach, the O_3 produced by LPG source before and after the program were obtained (Figure 6). Since O_3 formation was usually limited by VOCs and suppressed by NO titration, the VOCs and NO in LPG made positive and negative contributions to O_3 production, respectively. Considering the combined effect of VOCs and NO on O_3 formation, LPG generally made a net positive contribution to O_3. However, the contribution of LPG vehicle to O_3 formation at roadside sites was negative before the program, mainly due to higher levels of NO emitted from LPG-fueled vehicles (0.66±0.28 μg/m^3) than those at urban (0.34±0.42 μg/m^3) and new town sites (0.14±0.12 μg/m^3), resulting in higher NO titration to O_3.

Table 5 lists the average contributions of LPG vehicle exhaust to O_3 at different types of sites

before and after the replacement program. At the roadside sites, the contribution of LPG vehicle turned from O_3 destruction (-0.17±0.06 ppbv) before to O_3 formation (0.004±0.038 ppbv) after the program. However, the resulting O_3 increase was minor (only 0.18 ppbv, 3.1% of the average roadside O_3 value). Although the decrease of VOCs and NO was not significant at the urban sites (p>0.05), O_3 produced by LPG source decreased significantly (p<0.05), reflecting nonlinear relationship between O_3 and its precursors, and also indicating the effectiveness of the program on O_3 production at urban sites. At the new town sites, no significant change in the contribution of LPG vehicle to O_3 production were observed (p>0.05).

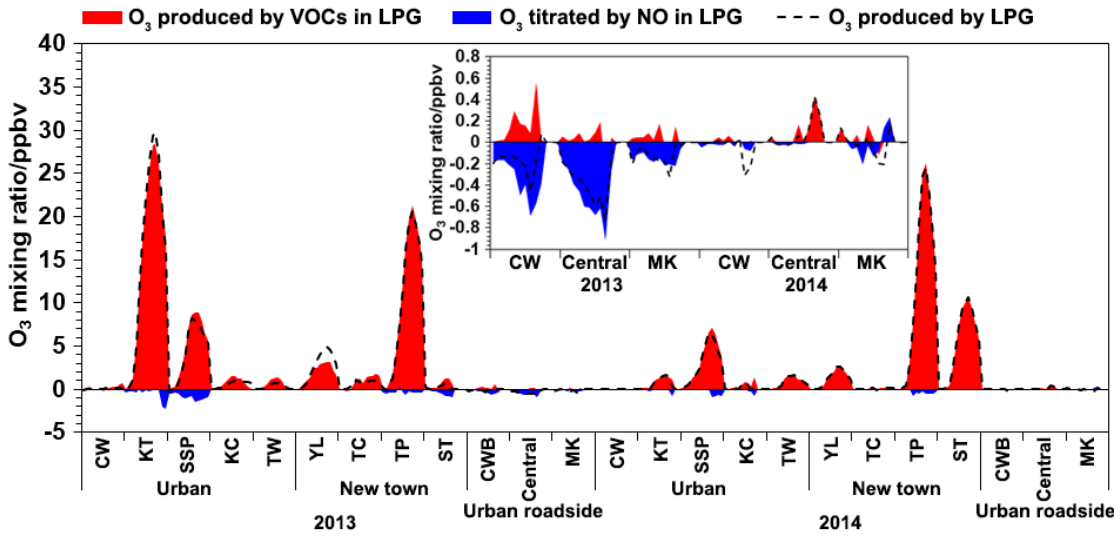

Figure 6 Contribution of LPG vehicle exhaust to O_3 production before and after the program. O_3 production by LPG at the roadside sites is enlarged in the insert panel.

Table 5 Site-dependent average contributions of LPG vehicle exhaust to O_3 production (Unit: ppbv)

	Before	After
Urban roadside	-0.17 ± 0.06	0.004 ± 0.038
Urban	4.19 ± 1.92	0.95 ± 0.38
New town	3.37 ± 1.56	4.47 ± 1.89

3.5 Spatial characteristics of O_3-precursor relationship

Figure 7 shows the relative incremental reactivity (RIR) of anthropogenic VOCs (AHC), biogenic VOCs (BHC), CO and NO_x, as a measure of the sensitivity of O_3 formation to the

changes of the precursors (Cardelino and Chameides, 1995). The VOC groups and CO had positive RIR values, and the RIR values of VOC groups were higher than that of CO, indicating that O_3 production was VOC-limited. The RIR values of AHC were mostly the highest, followed by BHC and CO. In contrast, the average RIR for NO_x was negative, suggesting that cutting NO_x led to O_3 increase. Different from other sites where O_3 formation was limited by AHC, BHC at the rural site TM was the most predominant reagent limiting O_3 formation in September 2013, whereas the RIR of NO_x in September 2014 became positive, same as VOCs and CO, indicating that O_3 formation was limited by both VOCs and NO_x. To understand the dominant VOC groups/species responsible for O_3 formation, Table 6 shows the average RIR values of VOC groups/species at different types of sites (The RIR value of each VOC species is given in Table S4). The alkenes (6.91) and aromatics (7.01) had comparable RIR values and were the highest at the roadside sites, indicating that vehicular emissions were the most important sources of O_3 formation at roadside sites. On the other hand, the aromatics at the urban and new town sites were the most predominant VOCs for O_3 formation, with the RIR values of 20.48 and 24.15, respectively. Solvent usage and traffic emissions were likely the main contributors at these two types of sites. In contrast, isoprene was responsible for O_3 formation at rural site with the RIR of 19.38.

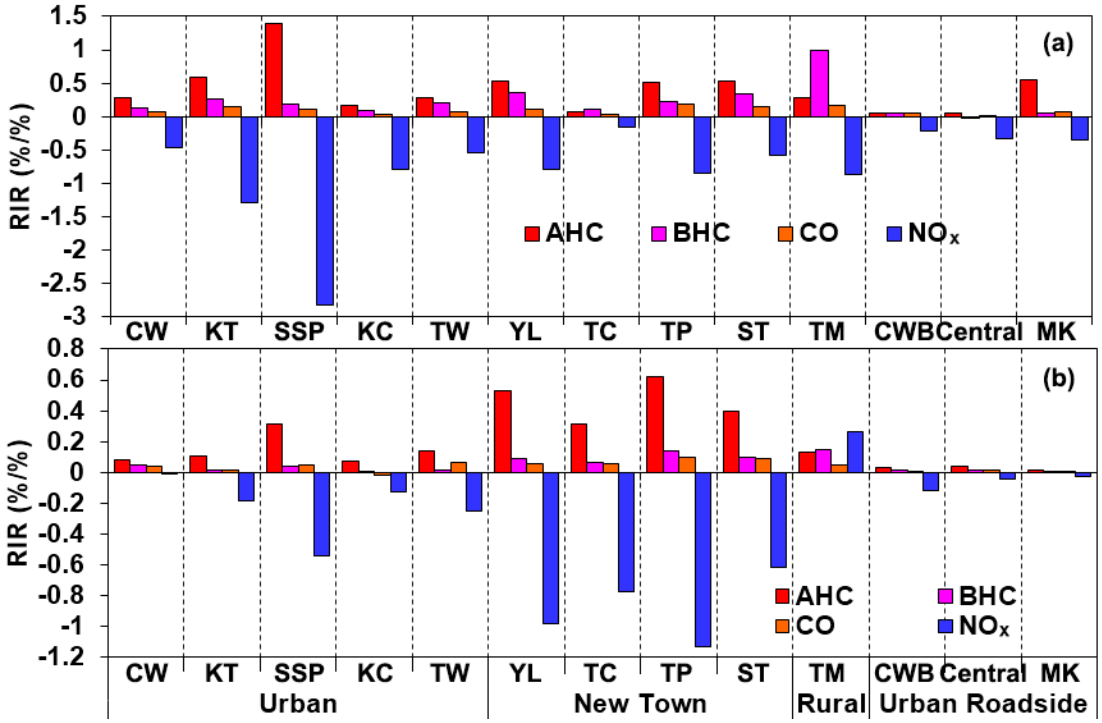

Figure 7 RIR values of VOC groups, CO and NO_x at different sites on (a) 27 Sept. 2013 and (b) 24 Sept. 2014

Table 6 Average RIR of VOC groups or species at different sites (Unit: %/%)

	Urban roadside	Urban	New town	Rural
Alkanes	4.22	8.72	9.67	7.98
Alkenes	**6.91**	10.24	11.35	8.35
Aromatics	**7.01**	**20.48**	**24.15**	15.19
Isoprene	1.31	4.18	8.56	**19.38**
Ethyne	0.02	0.19	0.31	0.81

4 Conclusions

VOC canister samples were collected at 30 sites in Hong Kong before and after the LPG converter replacement program. Source apportionment revealed that the VOCs emitted from LPG-fueled vehicles significantly decreased at urban roadside sites after the program, while they remained unchanged at urban and new town sites. LPG vehicle exhaust was destructive to O_3 formation at the roadside sites before the program, whereas it switched to positive contribution after the program. Nevertheless, the resulting O_3 increase was minor (3.1%). Although the decrease of VOCs and NO in LPG emissions was insignificant at the urban sites, O_3 produced by

LPG vehicle reduced significantly during the program. The above results confirmed the success of the program, particularly in roadside and urban environments. Furthermore, O_3 formation was mainly limited by VOCs regardless of locations, while VOCs and NO_x could co-control the O_3 formation in rural areas. In addition, anthropogenic VOCs were the main species dominating O_3 formation, *i.e.*, alkenes and aromatics in urban roadside environments, and aromatics at urban and new town sites, while O_3 formation at rural sites was most sensitive to biogenic VOCs. The spatial characteristics of O_3-precursor relationships provided useful guideline for the formulation and implementation of O_3 abatement strategies in different-function areas of Hong Kong.

Acknowledgments

We thank HKEPD for providing us the data. This study was supported by the Research Grants Council of the Hong Kong Special Administrative Region via grants (PolyU5154/13E, PolyU152052/14E, CRF/C5022-14G and CRF/C5004-15E), the HKPolyU PhD scholarship (project #RTUP), and the HKPolyU internal grants (1-ZVCX and G-YBHT). This study is partly supported by the National Natural Science Foundation of China (41275122).

References

Alicke B, Geyer A, Hofzumahaus A, Holland F, Konrad S, Pätz HW, et al. OH formation by HONO photolysis during the BERLIOZ experiment. Journal of Geophysical Research-Atmospheres 2003; 108: PHO 3-1-PHO 3-17.

Borbon A, Locoge N, Veillerot M, Galloo JC, Guillermo R. Characterisation of NMHCs in a French urban atmosphere: overview of the main sources. Science of the Total Environment 2002; 292: 177-191.

Cardelino C. Daily Variability of Motor Vehicle Emissions Derived from Traffic Counter Data. Journal of Air & Waste Management Association 1998; 48: 637-645.

Cardelino CA, Chameides WL. An Observation-Based Model for Analyzing Ozone Precursor Relationships in the Urban Atmosphere. Journal of Air & Waste Management Association 1995; 45: 161-180.

406 Censtatd. Census and Statistics Department HKG. Geography and climate, Hong Kong.
407 http://www.censtatd.gov.hk/FileManager/EN/Content_810/geog.pdf retrieved 27 January 2016.
408 Cheng HR, Guo H, Saunders SM, Lam SHM, Jiang F, Wang XM, et al. Assessing photochemical
409 ozone formation in the Pearl River Delta with a photochemical trajectory model. Atmospheric
410 Environment 2010a; 44: 4199-4208.
411 Cheng HR, Guo H, Wang XM, Saunders SM, Lam SHM, Jiang F, et al. On the relationship
412 between ozone and its precursors in the Pearl River Delta: application of an observation-based
413 model (OBM). Environmental Science and Pollution Research 2010b; 17: 547-560.
414 Colman JJ, Swanson AL, Meinardi S, Sive BC, Blake DR, Rowland FS. Description of the
415 Analysis of a Wide Range of Volatile Organic Compounds in Whole Air Samples Collected
416 during PEM-Tropics A and B. Analytical Chemistry 2001; 73: 3723-3731.
417 Creilson JK, Fishman J, Wozniak AE. Intercontinental transport of tropospheric ozone: a study of
418 its seasonal variability across the North Atlantic utilizing tropospheric ozone residuals and its
419 relationship to the North Atlantic Oscillation. Atmospheric Chemistry and Physics 2003; 3:
420 2053-2066.
421 Guenther AB. Modeling biogenic volatile organic compound emissions to the atmosphere. In
422 *Reactive hydrocarbons in the atmosphere*, Nicholas Hewitt editted. Elsevier Inc., London,
423 1999: 98-116.
424 Guenther AB, Zimmerman PR, Harley PC, Monson RK, Fall R. Isoprene and monoterpene
425 emission rate variability: Model evaluations and sensitivity analyses. Journal of Geophysical
426 Research-Atmospheres 1993; 98: 12609-12617.
427 Guo H, Cheng HR, Ling ZH, Louie PKK, Ayoko GA. Which emission sources are responsible
428 for the volatile organic compounds in the atmosphere of Pearl River Delta? Journal of
429 Hazardous Materials 2011a; 188: 116-124.
430 Guo H, So KL, Simpson IJ, Barletta B, Meinardi S, Blake DR. C-1-C-8 volatile organic
431 compounds in the atmosphere of Hong Kong: Overview of atmospheric processing and source

apportionment. Atmospheric Environment 2007; 41: 1456-1472.

Guo H, Wang T, Blake DR, Simpson IJ, Kwok YH, Li YS. Regional and local contributions to ambient non-methane volatile organic compounds at a polluted rural/coastal site in Pearl River Delta, China. Atmospheric Environment 2006; 40: 2345-2359.

Guo H, Zou SC, Tsai WY, Chan LY, Blake DR. Emission characteristics of nonmethane hydrocarbons from private cars and taxis at different driving speeds in Hong Kong. Atmospheric Environment 2011b; 45: 2711-2721.

HKEPD. Characterisation of VOC Sources and Integrated Photochemical Ozone Analysis in Hong Kong and the Pearl River Delta region. Internal Report, 2013.

HKEPD. Pearl River Delta Regional Air Quality Monitoring Network Report http://www.epd.gov.hk/epd/english/resources_pub/publications/m_report.html 2015a.

HKEPD. Hong Kong Air Pollutant Emission Inventory. http://www.epd.gov.hk/epd/english/environmentinhk/air/data/emission_inve.html 2015b.

Ho KF, Lee SC, Ho WK, Blake DR, Cheng Y, Li YS, et al. Vehicular emission of volatile organic compounds (VOCs) from a tunnel study in Hong Kong. Atmospheric Chemistry and Physics 2009; 9: 7491-7504.

Holzworth GC. Mixing Depths, Wind Speeds and Air Pollution Potential for Selected Locations in the United States. Journal of Applied Meteorology 1967; 6: 1039-1044.

Jacobson MZ. Fundamentals of Atmospheric Modelling: Cambridge University Press, 2005.

Jenkin ME, Clemitshaw KC. Ozone and other secondary photochemical pollutants: chemical processes governing their formation in the planetary boundary layer. Atmospheric Environment 2000; 34: 2499-2527.

Kleffmann J, Gavriloaiei T, Hofzumahaus A, Holland F, Koppmann R, Rupp L, et al. Daytime formation of nitrous acid: A major source of OH radicals in a forest. Geophysical Research Letters 2005; 32.

Lam SHM, Saunders SM, Guo H, Ling ZH, Jiang F, Wang XM, et al. Modelling VOC source

458 impacts on high ozone episode days observed at a mountain summit in Hong Kong under the
459 influence of mountain-valley breezes. Atmospheric Environment 2013; 81: 166-176.
460 Lam WHK, Tang YF, Chan KS, Tam ML. Short-term hourly traffic forecasts using Hong Kong
461 Annual Traffic Census. Transportation 2006; 33: 291-310.
462 Lau AKH, Yuan ZB, Yu JZ, Louie PKK. Source apportionment of ambient volatile organic
463 compounds in Hong Kong. Science of the Total Environment 2010; 408: 4138-4149.
464 Li Y, Lau AKH, Fung JCH, Ma H, Tse YY. Systematic evaluation of ozone control policies using
465 an Ozone Source Apportionment method. Atmospheric Environment 2013; 76: 136-146.
466 Li Y, Lau AKH, Fung JCH, Zheng JY, Zhong LJ, Louie PKK. Ozone source apportionment
467 (OSAT) to differentiate local regional and super-regional source contributions in the Pearl
468 River Delta region, China. Journal of Geophysical Research-Atmospheres 2012; 117.
469 Ling ZH, Guo H, Cheng HR, Yu YF. Sources of ambient volatile organic compounds and their
470 contributions to photochemical ozone formation at a site in the Pearl River Delta, southern
471 China. Environmental Pollution 2011; 159: 2310-2319.
472 Ling ZH, Guo H, Lam SHM, Saunders SM, Wang T. Atmospheric photochemical reactivity and
473 ozone production at two sites in Hong Kong: Application of a Master Chemical Mechanism-
474 photochemical box model. Journal of Geophysical Research-Atmospheres 2014; 119.
475 Ling ZH, Guo H, Zheng JY, Louie PKK, Cheng HR, Jiang F, Cheung K, Wong LC, Feng XQ.
476 Establishing a conceptual model for photochemical ozone pollution in subtropical Hong Kong.
477 Atmospheric Environment 2013; 76: 208-220.
478 Louie PKK, Ho JWK, Tsang RCW, Blake DR, Lau AKH, Yu JZ, et al. VOCs and OVOCs
479 distribution and control policy implications in Pearl River Delta region, China. Atmospheric
480 Environment 2013; 76: 125-135.
481 Lu K, Zhang Y. Observations of HOx Radical in Field Studies and the Analysis of Its Chemical
482 Mechanism. Progress in Chemistry 2010; 22: 500-514.
483 Lyu XP, Chen N, Guo H, Zhang WH, Wang N, Wang Y, et al. Ambient volatile organic

484 compounds and their effect on ozone production in Wuhan, central China. Science of the Total
485 Environment 2016; 541: 200-209.
486 Lyu XP, Guo H, Simpson IJ, Meinardi S, Louie PKK, Ling ZH, et al. Effectiveness of replacing
487 catalytic converters in LPG-fueled vehicles in Hong Kong. Atmospheirc Chemistry and
488 Physics Discussion 2015a; 15: 35939-35990.
489 Lyu XP, Ling ZH, Guo H, Saunders SM, Lam SHM, Wang N, et al. Re-examination of C1–C5
490 alkyl nitrates in Hong Kong using an observation-based model. Atmospheric Environment
491 2015b; 120: 28-37.
492 Mao JQ, Ren XR, Chen SA, Brune WH, Chen Z, Martinez M, et al. Atmospheric oxidation
493 capacity in the summer of Houston 2006: Comparison with summer measurements in other
494 metropolitan studies. Atmospheric Environment 2010; 44: 4107-4115.
495 Ou J, Guo H, Zheng J, Cheung K, Louie PKK, Ling Z, et al. Concentrations and sources of non-
496 methane hydrocarbons (NMHCs) from 2005 to 2013 in Hong Kong: A multi-year real-time
497 data analysis. Atmospheric Environment 2015; 103: 196-206.
498 Paatero P. Least squares formulation of robust non-negative factor analysis. Chemometrics and
499 Intelligent Laboratory Systems 1997; 37: 23-35.
500 Paatero P, Tapper U. Positive matrix factorization: A non-negative factor model with optimal
501 utilization of error estimates of data values. Environmetrics 1994; 5: 111-126.
502 Ren X, Brune WH, Oliger A, Metcalf AR, Simpas JB, Shirley T, et al. OH, HO2, and OH
503 reactivity during the PMTACS–NY Whiteface Mountain 2002 campaign: Observations and
504 model comparison. Journal of Geophysical Research-Atmospheres 2006; 111: D10.
505 Ren XR, van Duin D, Cazorla M, Chen S, Mao JQ, Zhang L, et al. Atmospheric oxidation
506 chemistry and ozone production: Results from SHARP 2009 in Houston, Texas. Journal of
507 Geophysical Research-Atmospheres 2013; 118: 5770-5780.
508 Seinfeld JH, Pandis SN. Atmospheric Chemistry and Physics: From Air Pollution to Climate
509 Change. John Wiley & Sons, Inc., 1997.

510 Simpson IJ, Blake NJ, Barletta B, Diskin GS, Fuelberg HE, Gorham K, et al. Characterization of
511 trace gases measured over Alberta oil sands mining operations: 76 speciated C-2-C-10 volatile
512 organic compounds (VOCs), CO2, CH4, CO, NO, NO2, NOy, O3 and SO2. Atmospheric
513 Chemistry and Physics 2010; 10: 11931-11954.
514 Sommariva R, Haggerstone AL, Carpenter LJ, Carslaw N, Creasey DJ, Heard DE, et al. OH and
515 HO2 chemistry in clean marine air during SOAPEX-2. Atmospheric Chemistry and Physics
516 2004; 4: 839-856.
517 USEPA. EPA Positive Matrix Factorization (PMF) 3.0 Fundamentals & User Guide.
518 www.epa.gov 2008.
519 USEPA. User's Guide for the Industrial Source Complex (ISC3) Dispersion Models, Volume II
520 Description of Model Algorithms. EPA-454/B-95-003b. U.S. Environmental Protection
521 Agency, Research Triangle Park, NC. 1985.
522 Wang J-L, Wang C-H, Lai C-H, Chang C-C, Liu Y, Zhang Y, et al. Characterization of ozone
523 precursors in the Pearl River Delta by time series observation of non-methane hydrocarbons.
524 Atmospheric Environment 2008; 42: 6233-6246.
525 Wang T, Wei XL, Ding AJ, Poon CN, Lam KS, Li YS, et al. Increasing surface ozone
526 concentrations in the background atmosphere of Southern China, 1994–2007. Atmospheric
527 Chemistr and Physics 2009; 9: 6217-6227.
528 WebMET. Met Monitoring Guide, The Meteorological Resource Center.
529 http://www.webmet.com/met_monitoring/622.html accessed on 30 July 2015 2015; 6.2.2
530 Vector computations.
531 Xia L, Shao Y. Modelling of traffic flow and air pollution emission with application to Hong
532 Kong Island. Environmental Modelling & Software 2005; 20: 1175-1188.
533 Xue LK, Wang T, Guo H, Blake DR, Tang J, Zhang XC, et al. Sources and photochemistry of
534 volatile organic compounds in the remote atmosphere of western China: results from the Mt.
535 Waliguan Observatory. Atmospheric Chemistry and Physics 2013; 13: 8551-8567.

536 Xue LK, Wang T, Louie PKK, Luk CWY, Blake DR, Xu Z. Increasing External Effects Negate
537 Local Efforts to Control Ozone Air Pollution: A Case Study of Hong Kong and Implications
538 for Other Chinese Cities. Environmental Science & Technology 2014; 48: 10769-10775.
539 Xue LK, Wang T, Zhang JM, Zhang XC, Deliger, Poon CN, et al. Source of surface ozone and
540 reactive nitrogen speciation at Mount Waliguan in western China: New insights from the 2006
541 summer study. Journal of Geophysical Research-Atmospheres 2011; 116: D07306.
542 Zhang J, Wang T, Chameides WL, Cardelino C, Kwok J, Blake DR, et al. Ozone production and
543 hydrocarbon reactivity in Hong Kong, Southern China. Atmospheric Chemistry and Physics
544 2007; 7: 557-573.

Supplementary material for on-line publication only

Click here to download Supplementary material for on-line publication only: Supplementary material_Submitted.docx